Table 1
Transmission of various human prions to both knock-in mice and transgenic mice via intracerebral route and the resulting positivity of PrP^{Sc} observed in lymphoid organs

Recipient mouse line	Expression	Inoculum	Incubation period	Spleen	LN	Peyer
Ki-ChM (PrnpChM/ChM)	1x	sCJD (H-3)	151 ± 6.7(7/7)	(5/5)	(4/4)	(3/3)
Ki-ChM (PrnpChM/ChM)	1x	iCJD (Du/c)	167 ± 24.7(6/6)	(5/5)		(4/4)
Ki-ChM (PrnpChM/ChM)	1x	fCJD (TM232)	177 ± 4.9(4/4)	(4/4)	(3/3)	(3/4)
Ki-ChM (PrnpChM/ChM)	1x	sCJD (Sumi)	141 ± 5.3(5/5)	(4/4)	(4/4)	(4/4)
Tg-ChM#30 (Prnp0/0)	0.7x	sCJD (H-3)	156 ± 14.2(11/11)	(0/8)	(0/6)	(0/4)
Tg-ChM#30 (Prnp0/0)	0.7x	fCJD (TM232)	179 ± 13.1(5/5)	(0/3)	(0/3)	(0/3)
Tg-ChM#30 (Prnp0/0)	0.7x	sCJD (Phily)	154 ± 20.4(5/5)	(0/5)	(0/5)	(0/5)
Tg-ChV#12 (Prnp0/0)	2x	sCJD (H-3)	175 ± 15.3(18/18)	(0/18)	(2/12)	(2/7)
Tg-ChV#12 (Prnp0/0)	2x	iCJD (Du/c)	189 ± 6.4(6/6)	(0/4)	(1/3)	(0/3)
Tg-ChV#12 (Prnp0/0)	2x	fCJD (TM232)	220 ± 8.7(3/3)	(0/3)	(0/2)	(0/2)
Tg-ChV#12 (Prnp0/0)	2x	sCJD (Phily)	171 ± 9.2(10/10)	(0/6)	(0/4)	(0/5)
Tg-ChV#21 (Prnp0/0)	4x	sCJD (H-3)	192 ± 4.0(3/3)	(1/3)	(0/2)	(0/2)
Tg-ChV#21 (Prnp0/0)	4x	sCJD (Phily)	188 ± 1.4(2/2)	(0/2)		(0/2)

PrnpChM/ChM, homozygous knock-in mice with chimeric PrP; (Prnp0/0), ablated PrP background mice, sCJD: sporadic CJD, iCJD: iatrogenic CJD, fCJD: familial CJD, H-3: codon 129 Met/Met and type 1 PrP^{Sc} (MM1) [31], Du/c: dura-associated CJD with MM1, TM232: codon 232 mutation, Sumi: MV1, Phily: MV2, incubation period: means ± SD days post-inoculation (transmitted mice/total mice), spleen; LN (lymph nodes); Peyer (Peyer's patches): positivity of immunostained PrP^{Sc} in the follicular dendritic cells (number of positive mice/number of the examined mice).

CJD (fCJD). These homogenates were inoculated intracerebrally into the model mice. Ki-ChM ($Prnp^{ChM/ChM}$) mice were highly susceptible to human prions. Tg-ChM#30 ($Prnp^{0/0}$) mice also possessed short incubation periods. Thus, ChM chimeric PrP demonstrated highly susceptible models for human prions as reported in Tg(MHu2M) mouse [24]. Therefore, C-terminal part of mouse PrP sequence is clearly important for the conversion of humanized PrP. Interestingly, Tg-ChV#21 ($Prnp^{0/0}$, expression level; 4x) demonstrated longer incubation periods than Tg-ChV#12mice ($Prnp^{0/0}$, expression level; 2x), following inoculation with sCJD human prions. In our chimeric PrP construct, overexpression did not shorten the incubation periods seen in transgenic mice expressing wild type PrP [25,26].

PrP^{Sc} in the follicular dendritic cells of humanized mice

Immunohistochemical analysis of lymphoid organs with an anti-PrP antibody revealed PrP^{Sc} staining of FDC in the spleens, lymph nodes, and intestinal Peyer's patches in Ki-ChM mice at the onset of disease (Table 1 and Fig. 2A). In the spleens, 100% of the Ki-ChM mice was positive for anti-PrP staining. Positive immunohistochemical results were confirmed by Western blot analysis. Protease-resistant PrP^{Sc} molecules were detected in the spleens of infected Ki-ChM mice, but not in uninfected Ki-ChM mice (Fig. 2B). In contrast, none of the Tg-ChM#30 or Tg-ChV#12 mice was positive in the spleen; one of Tg-ChV#21 mice demonstrated positive reactions in the spleen (Table 1).

The absence of PrP^{Sc} in the FDC of transgenic mice is ascribed to the level of recombinant PrP expression. The expression of recombinant PrP^{C} in the membrane fraction of the spleen estimated that the Tg-ChV#12 ($Prnp^{0/0}$) mouse possessed only <25% of that expressed in the Ki-ChM ($Prnp^{ChM/ChM}$) mouse (Fig. 3A). Immuno-histochemistry revealed positive PrP^{C} expression in splenic FDC of the Ki-ChM mice; this staining was absent from Tg-ChV#12 mice (Fig. 3B). Thus, our transgenic vector led to attenuated or ectopic expression of recombinant PrP in the spleen, in agreement with evidence describing the dependence of scrapie replication in lymphoid tissues on the existence of PrP^{C}-expressing FDC [27].

Sequential analysis in the follicular dendritic cells

Ki-ChM ($Prnp^{ChM/ChM}$) mice were inoculated intraperitoneally with 50 μl of 10% homogenate of human sCJD prions. The number of Ki-ChM mice demonstrating positive splenic FDC immunoreactivity increased with prolonged incubation time; 100% of Ki-ChM mice had positive splenic FDC staining at 30 days post-inoculation (Table 2). Positive FDC stainings of the lymph nodes or Peyer's patches developed slowly. All Ki-ChM mice demonstrated positive FDC immunoreactivity in the lymph nodes 60 days post-inoculation; immunoreactivity of all mice appeared in Peyer's patches 75 days post-inoculation. FDC of NZW mice provided a rapid bioassay system for mouse prions [10]; in the same manner, FDC in Ki-ChM mice provide such a system for human prions.

Bioassay for various human prion diseases

We utilized this FDC assay system to examine various human prion diseases (Table 3). The inoculum consisted of a 10% homogenate of brain tissue prepared from patients with sCJD, iCJD, or vCJD. Two cases of Alzheimer's disease, an unrelated neurodegenerative disease causing dementia, were used as a control. Fifty μl of

Fig. 2. Abnormal PrP in the spleen of the knock-in mouse. (A) Immunohistochemical stainings for PrP in the spleens of the Ki-ChM mice, inoculated intracerebrally with sporadic CJD (H-3). Positive labeling is observed in follicular dendritic cells. Anti-PrP–N antiserum was used as the primary antibody. Bar shows 0.7 mm in a low magnified figure, bar shows 160 μm in a high magnified one. (B) Western blot analysis of the spleen and brain of Ki-ChM mice inoculated intracerebrally with sporadic CJD (H-3). Protease-resistant PrP is detected in the spleen of the infected Ki-ChM mice (Lane 1), but not in the uninfected mice (Lane 2). Protease-resistant PrP from the brain of infected Ki-ChM mice is also immunolabeled as a positive control (Lane Br). Anti-APC was used as the primary antibody recognizing PrP. The numbers, 32.5 and 25, designate the approximate molecular sizes (kDa).

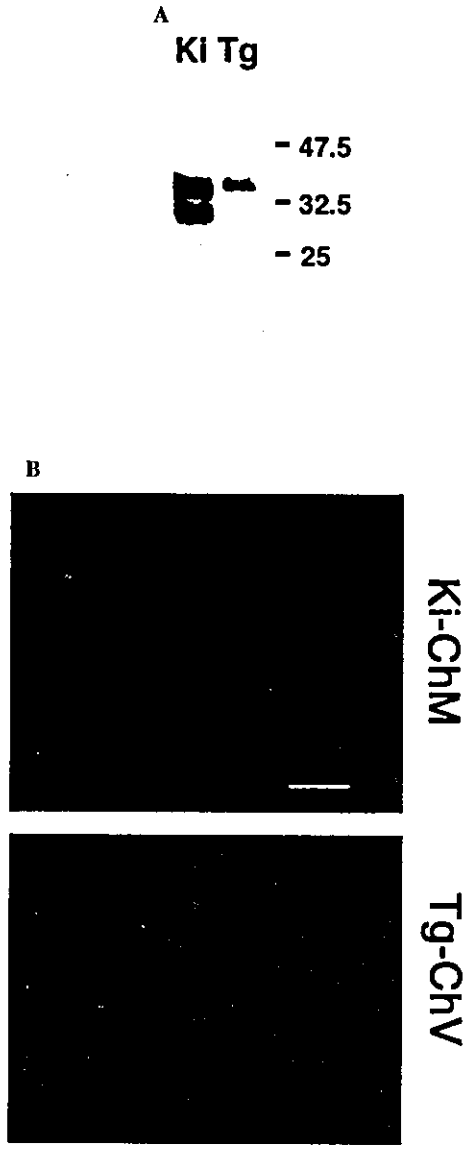

Fig. 3. Recombinant PrP expression in the spleen of the knock-in or the transgenic mice. (A) Western blot analysis of PrP^{C} in the uninfected mice. The splenic membrane fractions isolated from 10 mg of wet weight tissue was probed with anti-PrP–N. The fraction isolated from Ki-ChM ($Prnp^{ChM/ChM}$) mice possesses stronger immunoreactivity (Lane Ki) than fractions derived from Tg-ChV#12 ($Prnp^{0/0}$) mice (Lane Tg). The numbers, 47.5, 32.5, and 25, denote the molecular sizes (kDa). (B) Immunofluorescent analysis of the spleen with anti-PrP–N. Positive reactivity is observed in follicular dendritic cells of Ki-ChM mice, not in Tg-ChV mice. Bar shows 100 μm. Both figures have the same magnification.

each homogenate was inoculated into the peritoneum of Ki-ChM ($Prnp^{ChM/ChM}$) mice. The mice were sacrificed 75 days after the inoculation because of full-blown PrP^{Sc} accumulations observed at this stage in the sequential analysis (Table 2). We detected PrP^{Sc} in the splenic FDC following inoculation with samples from patients with either sCJD or iCJD. This bioassay system also provides a valuable analysis of vCJD prions. We could detect PrP^{Sc} in the splenic FDC of all mice inoculated with vCJD prions. No positive FDC staining was obtained for samples from patients with Alzheimer's disease. Thus, the positivity of PrP^{Sc} in the splenic FDC correlates with the presence of PrP^{Sc} in the human brain inoculum. Therefore, it is intriguing to know whether PrP^{Sc} seen in the FDC is simply collected from human brain inoculum or not.

The origin of PrP^{Sc} accumulated in the follicular dendritic cells

To determine whether the PrP^{Sc} found in FDC resulted from the accumulations collected from the inoculated human samples (human PrP^{Sc}) or from

Table 2
Sequential transmission to Ki-ChM mice via intraperitoneal route and positivity of PrP^{Sc} observed in lymphoid organs

Post-inoculation days	Spleen	LN	Peyer
14	(2/4)	(1/3)	(0/3)
30	(6/6)	(4/6)	(0/4)
45	(7/7)	(4/5)	(4/6)
60	(6/6)	(3/3)	(5/6)
75	(5/5)	(5/5)	(4/4)
150	(7/7)	(7/7)	(6/6)

Ki-ChM mice received intraperitoneal inoculation of brain homogenates from sCJD patients (H-3; MM1). Mice were sacrified at variable days post-inoculation. Positivity of immunoreactive PrP^{Sc} in the spleen, lymph node (LN), or Peyer's patches (Peyer) is denoted as the number of positive mice/number of total mice examined.

Table 3
Transmission of human prions or brains affected with Alzheimer's disease to Ki-ChM mice and positivity of PrP^{Sc} in the spleen

Inoculum	Spleen
sCJD (H-3)	(7/7)
sCJD (Sumi)	(5/5)
iCJD (Du/c)	(6/6)
vCJD (96/02)	(5/5)
vCJD (96/07)	(4/4)
vCJD (96/45)	(6/6)
AD (H3982)	(0/4)
AD (H4023)	(0/7)

Ki-ChM (PrnpChM/ChM) mice received intraperitoneal inoculation of 10% brain homogenates prepared from patients with either sporadic CJD (sCJD), iatrogenic CJD (iCJD), variant CJD (vCJD), or Alzheimer's disease (AD). Mice were sacrificed 75 days post-inoculation. H-3: MM1, Sumi: MV1, Du/c: dura-associated CJD with MM1, 96/02: MM2* [32] or MM4 [33], 96/07: MM2*/MM4, 96/45: MM2*/MM4, H3982: codon 129M/M and codon 219E/E without PrP^{Sc}, H4023: codon 129M/M and codon 219E/E without PrP^{Sc}. Spleen: positivity in the follicular dendritic cells of the spleen (number of positive mice/ number of total mice examined).

newly converted PrP^{Sc} of Ki-ChM mice (recombinant PrP^{Sc}), we stained spleens with a monoclonal antibody, TNT#71, specific for the C-terminal sequence of human PrP. The TNT#71 recognizes human PrP containing 215Ile, 219Glu, and 220Arg, but does not recognize mouse PrP with codons 214Val, 218Gln, and 219Lys [20]. This specific recognition of human PrP, not of chimeric PrP in the Ki-ChM mouse, enables the differential examination of PrP^{Sc} depositions in splenic FDC following inoculation with human samples. Positive reactivity of the splenic FDC in Ki-ChM mouse was obtained with the 3F4 antibody, but not with the TNT#71 antibody (Fig. 4). As a positive control, TNT#71 antibody reacted with the FDC in the tonsil of a patient with vCJD. Therefore, the PrP^{Sc} seen in the splenic FDC of Ki-ChM mice was not derived from the inoculated human PrP^{Sc}, but from the recombinant PrP^{Sc}.

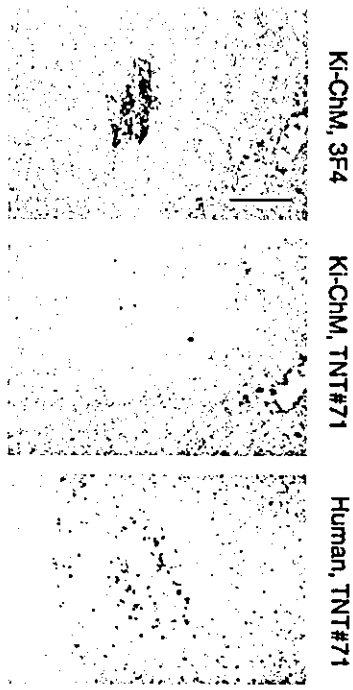

Fig. 4. Immunohistochemical analysis in the PrP^{Sc} of the spleen with 3F4 and TNT#71monoclonal antibodies. PrP^{Sc} seen in follicular dendritic cells of Ki-ChM mice, inoculated with vCJD prions, is positively immunolabeled by the 3F4 antibody, but not by the TNT#71 antibody. Human tonsilar FDC was the positive control for TNT#71 immunostaining. Bar shows 120 μm. All figures have the same magnification.

Serial passage to Ki-ChM mice

For the titration of infectivity, the second passaged brains of Ki-ChM mouse were homogenized and were inoculated intracerebrally with serial dilutions (Table 4). The titer of the brain tissues was 8.16 log LD_{50} U/g that was calculated by the incubation time method [28] using the relation; $y = 13.79 - 0.063x$ (R^2; 0.9124), where y is the log LD_{50} and x is the incubation time (in days) to terminal disease. When one or more animals survived >240 days, the titer was assumed to be close to the end point. We examined the infectivity of the brain from the first-passaged Ki-ChM mouse, demonstrating ~123 days incubation period (6.04 log LD_{50}).

We also analyzed the infectivity of the spleen isolated from the first passaged Ki-ChM mouse or the first passaged Tg-ChM#30 mouse. The serial transmission of the Ki-ChM spleen tissues demonstrated ~156 days incubation periods (3.96 log LD_{50}), but the transmission of the Tg-ChM#30 spleen tissues showed a faint infectivity (<2.16 log LD_{50}) (Table 4). Thus, negative FDC stainings in the spleens of Tg-ChM#30 mice indeed corresponded to the low titer of the spleen infectivity.

Table 4
Serial passage studies of human prions inoculated into Ki-ChM mice

Original source	Route	Inoculum	Incubation	Titers
sCJD	Ic	H-3→ Ki-ChM (brain)	123 ± 10.0 (6/6)	6.04
sCJD	Ic	H-3→ Ki-ChM (spleen)	156 ± 7.9 (5/5)	3.96
sCJD	Ic	H-3→ Tg-ChM#30 (spleen)	>295 (2/6)	<2.16
sCJD	Ic	H-3→ Ki-ChM (brain)→ Ki-ChM (brain)		
		homogenate 10^{-1}	109 ± 1.0 (6/6)	7.16
		homogenate 10^{-2}	121 ± 5.1 (6/6)	6.16
		homogenate 10^{-3}	139 ± 7.2 (4/4)	5.16
		homogenate 10^{-4}	149 ± 3.1 (5/5)	4.16
		homogenate 10^{-5}	167 ± 12.4 (6/6)	3.16
		homogenate 10^{-6}	240 ± 78.1 (4/5)	2.16
		homogenate 10^{-7}	319 (1/6)	1.16

sCJD: sporadic CJD, H-3: human prions (MM1), H-3 → Ki-ChM (brain or spleen): Ki-ChM prions for the second passage, H-3 → Ki-ChM (brain)→ Ki-ChM (brain): Ki-ChM prions for the third passage with serial dilution. Incubation period: Means ± S.D. days after the inoculation (number of transmitted mice/number of total mice). The titer of the brain tissues was 8.16 log LD_{50} U/g that was calculated by the incubation time method [28].

Discussion

To establish a new method examining transmissibility of human prions, a bioassay system should provide the early detection of humanized PrP^{Sc} and infectivity of PrP^{Sc}-positive organs. In Ki-ChM mice, we identified recombinant PrP^{Sc} in FDC after a 14 days incubation. We also detected the infectivity of spleens derived from first passaged Ki-ChM mice inoculated with sCJD prions. Thus, chimeric PrP in the FDC is readily converted into the infectious form. In previous vCJD transmission studies [29,30], transgenic mice with bovine PrP displayed incubation periods of ~270 days; transgenic mice with human PrP (codon 129 Val) demonstrated an incubation period of >228 days with a low transmission rate (25/56). Our bioassay system allowed for the detection of the recombinant PrP^{Sc} in the FDC of all the Ki-ChM mice inoculated with vCJD prions. This FDC detection system in Ki-ChM mice provides a rapid bioassay for the infectivity of human prions, including vCJD prions.

Intraperitoneal administration of the inoculum provides an advantage over intracerebral injection. Only a limited volume (20 μl) can be inoculated by the intracerebral route. To overcome this limitation, we employed an intraperitoneal administration, allowing repetitive injection of a volume up to ~2 ml. In addition, 50 μl of 10^7-diluted human sCJD homogenates showed a positive FDC stainings in 50% of inoculated Ki-ChM mice (unpublished data). Therfore, our FDC bioassay demonstrated a high sensitivity as the intracerebral transmission study did. Thus, enlarged sample volumes may result in the enhanced sensitivity of the bioassay to human materials with a low infectivity, such as blood derived from a patient or a healthy carrier with vCJD and pharmacological products made from human blood or organs.

Acknowledgments

We would like to thank J. Tateishi and H. Kudo for discussion and technical assistance. This study was supported by a grant from OPSR (T.K., S.M., I.M., and T.M.), a grant from the Ministry of Health, Labour, and Welfare (T.K., S.M., I.M., and T.T.), and a Grant-in-Aid for Scientific Research from the Ministry of Education, Culture, Sports, Science, and Technology (T.K., S.M., and T.M.).

References

[1] S.B. Prusiner, M.P. McKinley, K.A. Bowman, D.C. Bolton, P.E. Bendheim, D.F. Groth, G.G. Glenner, Scrapie prions aggregate to form amyloid-like birefringent rods, Cell 35 (1983) 349–358.
[2] S.B. Prusiner, Prions and neurodegenerative diseases, N. Engl. J. Med. 317 (1987) 1571–1581.
[3] C.M. Eklund, R.C. Kennedy, W.J. Hadlow, Pathogenesis of scrapie virus infection in the mouse, J. Infect. Dis. 117 (1967) 15–22.
[4] Y. Kuroda, C.J. Gibbs Jr., H.L. Amyx, D.C. Gajdusek, Creutzfeldt-Jakob disease in mice: persistent viremia and preferential replication of virus in low-density lymphocytes, Infect. Immunol. 41 (1983) 154–161.
[5] M. Shinagawa, E. Munekata, S. Doi, K. Takahashi, H. Goto, G. Sato, Immunoreactivity of a synthetic pentadecapeptide corresponding to the N-terminal region of the scrapie prion protein, J. Gen. Virol. 67 (1986) 1745–1750.
[6] S. Doi, M. Ito, M. Shinagawa, G. Sato, H. Isomura, H. Goto, Western blot detection of scrapie-associated fibril protein in tissues outside the central nervous system from preclinical scrapie-infected mice, J. Gen Virol. 69 (1988) 955–960.
[7] T. Kitamoto, S. Mohri, J. Tateishi, Organ distribution of proteinase-resistant prion protein in humans and mice with Creutzfeldt–Jakob disease, J. Gen. Virol. 70 (1989) 3371–3379.
[8] T. Kitamoto, T. Muramoto, S. Mohri, K. Doh-ura, J. Tateishi, Abnormal isoform of prion protein accumulates in follicular dendritic cells in mice with Creutzfeldt–Jakob disease, J. Virol. 65 (1991) 6292–6295.
[9] T. Muramoto, T. Kitamoto, J. Tateishi, I. Goto, The sequential development of abnormal prion protein accumulation in mice with Creutzfeldt–Jakob disease, Am. J. Pathol. 140 (1992) 1411–1420.

[10] T. Muramoto, T. Kitamoto, J. Tateishi, I. Goto, Accumulation of abnormal prion protein in mice infected with Creutzfeldt–Jakob disease via intraperitoneal route: a sequential study, Am. J. Pathol. 143 (1993) 1470–1479.
[11] L.J. van Keulen, B.E. Schreuder, R.H. Meloen, G. Mooij-Harkes, M.E. Vromans, J.P. Langeveld, Immunohistochemical detection of prion protein in lymphoid tissues of sheep with natural scrapie, J. Clin. Microbiol. 34 (1996) 1228–1231.
[12] B.E. Schreuder, L.J. van Keulen, M.E. Vromans, J.P. Langeveld, M.A. Smits, Preclinical test for prion diseases, Nature 381 (1996) 563.
[13] D.A. Hilton, E. Fathers, P. Edwards, J.W. Ironside, J. Zajicek, Prion immunoreactivity in appendix before clinical onset of variant Creutzfeldt-Jakob disease, Lancet 352 (1998) 703–704.
[14] T. Muramoto, T. Kitamoto, M.Z. Hoque, J. Tateishi, I. Goto, Species barrier prevents an abnormal isoform of prion protein from accumulating in follicular dendritic cells of mice with Creutzfeldt–Jakob disease, J. Virol. 67 (1993) 6808–6810.
[15] T. Kitamoto, K. Nakamura, K. Nakao, S. Shibuya, R.W. Shin, Y. Gondo, M. Katsuki, J. Tateishi, Humanized prion protein knock-in by Cre-induced site-specific recombination in the mouse, Biochem. Biophys. Res. Commun. 222 (1996) 742–747.
[16] K. Maki, I. Miyoshi, Y. Kon, T. Yamashita, N. Sasaki, S. Aoyama, E. Takahashi, S. Namioka, Y. Hayashizaki, N. Kasai, Targeted pituitary tumorigenesis using the human thyrotropin beta-subunit chain promoter in transgenic mice, Mol. Cell. Endocrinol. 105 (1994) 147–154.
[17] T. Yokoyama, K.M. Kimura, Y. Ushiki, S. Yamada, A. Morooka, T. Nakashiba, T. Sassa, S. Itohara, In vivo conversion of cellular prion protein to pathogenic isoforms, as monitored by conformation-specific antibodies, J. Biol. Chem. 276 (2001) 11265–11271.
[18] T. Kitamoto, M. Ohta, K. Doh-ura, S. Hitoshi, Y. Terao, J. Tateishi, Novel missense variants of prion protein in Creutzfeldt–Jakob disease or Gerstmann–Straussler syndrome, Biochem. Biophys. Res. Commun. 191 (1993) 709–714.
[19] T. Kitamoto, R.W. Shin, K. Doh-ura, N. Tomokane, M. Miyazono, T. Muramoto, J. Tateishi, Abnormal isoform of prion proteins accumulates in the synaptic structures of the central nervous system in patients with Creutzfeldt–Jakob disease, Am. J. Pathol. 140 (1992) 1285–1294.
[20] T. Muramoto, T. Tanaka, N. Kitamoto, C. Sano, Y. Hayashi, T. Kutomi, C. Yutani, T. Kitamoto, Analyses of Gerstmann–Sträussler syndrome with 102Leu219Lys using monoclonal antibodies that specifically detect human prion protein with 219Glu, Neurosci. Lett. 288 (2000) 179–182.
[21] T. Kitamoto, T. Muramoto, C. Hilbich, K. Beyreuther, J. Tateishi, N-terminal sequence of prion protein is also integrated into kuru plaques in patients with Gerstmann–Sträussler syndrome, Brain Res. 545 (1991) 319–321.
[22] K.U. Grathwohl, M. Horiuchi, N. Ishiguro, M. Shinagawa, Improvement of PrPSc-detection in mouse spleen early at the preclinical stage of scrapie with collagenase-completed tissue homogenization and Sarkosyl-NaCl extraction of PrP^{Sc}, Arch. Virol. 141 (1996) 1863–1874.
[23] T. Kitamoto, J. Tateishi, Immunohistochemical confirmation of Creutzfeldt–Jakob disease with a long clinical course with amyloid plaque core antibodies, Am. J. Pathol. 131 (1988) 435–443.
[24] G.C. Telling, M. Scott, K.K. Hsiao, D. Foster, S.L. Yang, M. Torchia, K.C. Sidle, J. Collinge, S.J. DeArmond, S.B. Prusiner, Transmission of Creutzfeldt–Jakob disease from humans to transgenic mice expressing chimeric human-mouse prion protein, Proc. Natl. Acad. Sci. USA 91 (1994) 9936–9940.
[25] S.B. Prusiner, M. Scott, D. Foster, K.M. Pan, D. Groth, C. Mirenda, M. Torchia, S.L. Yang, D. Serban, G.A. Carlson, S.J. DeArmond, Transgenetic studies implicate interactions between homologous PrP isoforms in scrapie prion replication, Cell 63 (1990) 673–686.
[26] J. Collinge, M.S. Palmer, K.C. Sidle, A.F. Hill, I. Gowland, J. Meads, E. Asante, R. Bradley, L.J. Doey, P.L. Lantos, Unaltered susceptibility to BSE in transgenic mice expressing human prion protein, Nature 378 (1995) 779–783.
[27] K.L. Brown, K. Stewart, D.L. Ritchie, N.A. Mabbott, A. Williams, H. Fraser, W.I. Morrison, M.E. Bruce, Scrapie replication in lymphoid tissues depends on prion protein-expressing follicular dendritic cells, Nat. Med. 5 (1999) 1308–1312.
[28] S.B. Prusiner, S.P. Cochran, D.F. Groth, D.E. Downey, K.A. Bowman, H.M. Martinez, Measurement of the scrapie agent using an incubation time interval assay, Ann. Neurol. 11 (1982) 353–358.
[29] M.R. Scott, R. Will, J. Ironside, H.O. Nguyen, P. Tremblay, S.J. DeArmond, S.B. Prusiner, Compelling transgenetic evidence for transmission of bovine spongiform encephalopathy prions to humans, Proc. Natl. Acad. Sci. USA 96 (1999) 15137–15142.
[30] A.F. Hill, M. Desbruslais, S. Joiner, K.C. Sidle, I. Gowland, J. Collinge, L.J. Doey, P. Lantos, The same prion strain causes vCJD and BSE, Nature 389 (1997) 448–450.
[31] P. Parchi, A. Giese, S. Capellari, P. Brown, W. Schulz-Schaeffer, O. Windl, I. Zerr, H. Budka, N. Kopp, P. Piccardo, S. Poser, A. Rojiani, N. Streichemberger, J. Julien, C. Vital, B. Ghetti, P. Gambetti, H. Kretzschmar, Classification of sporadic Creutzfeldt–Jakob disease based on molecular and phenotypic analysis of 300 subjects, Ann. Neurol. 46 (1999) 224–233.
[32] P. Parchi, S. Capellari, S.G. Chen, R.B. Petersen, P. Gambetti, N. Kopp, P. Brown, T. Kitamoto, J. Tateishi, A. Giese, H. Kretzschmar, Typing prion isoforms, Nature 386 (1997) 232–234.
[33] J. Collinge, K.C. Sidle, J. Meads, J. Ironside, A.F. Hill, Molecular analysis of prion strain variation and the aetiology of 'new variant' CJD, Nature 383 (1996) 685–690.

FULL PAPER *Clinical Pathology*

Amino Acid Polymorphisms of PrP Gene in Mongolian Sheep

Altangerel GOMBOJAV[1,2], Naotaka ISHIGURO[1], Motohiro HORIUCHI[1], Dorj SERJMYADAG[3], Badarch BYAMBAA[3] and Morikazu SHINAGAWA[1]

[1]*Laboratory of Veterinary Public Health, Obihiro University of Agriculture and Veterinary Medicine, Obihiro, Hokkaido 080–8555,* [2]*School of Veterinary Medicine, Biotechnology and* [3]*Institute of Veterinary Medicine, Mongolian State University of Agriculture, Ulaanbaatar 210153, Zaisan, Mongolia*

(Received 14 March 2002/Accepted 9 October 2002)

ABSTRACT. To characterize amino acid polymorphisms in sheep prion protein (PrP), we analyzed the PrP genes from 271 sheep of 4 breeds (Khalkh, Yeroo, Orkhon and Khangai) raised in central Mongolia (Tuv, Uvurkhangai and Selenge prefectures). A total of 16 genotypes and 8 allelic variants of the PrP gene at codons 112, 136, 154 and 171 were found. At codon 171, 1.8% of the sheep had arginine/arginine (R/R) (resistant to scrapie) and 66.8% had glutamine/glutamine (Q/Q) (susceptible to scrapie). Several Yeroo and Orkhon sheep raised in Selenge prefecture had valine at codon 136 (136V) (highly susceptible to scrapie). Several Yeroo, Orkhon and Khangai sheep raised in Selenge prefecture had histidine at codon 154 (154H). Novel polymorphisms of valine (V) and serine (S) at codon 127, lysine (K) at codon 171, and leucine (L) and arginine (R) at codon 189 were also found in Khalkh, Yeroo and Orkhon sheep. It is not known whether these novel polymorphisms affect scrapie susceptibility.

KEY WORDS: allelic frequency, PCR, PrP gene, RFLP, scrapie susceptibility.

J. Vet. Med. Sci. 65(1): 75–81, 2003

Scrapie is a fatal and infectious neurodegenerative disease occurring in sheep and goats. The primary cause of this disease is a post-translational conformational change in a host-encoded cellular protein known as prion protein (PrP), from wild type (PrP^C) to a partially proteinase-resistant form (PrP^{Sc}), in the presence of prion [25–27]. Polymorphisms in the PrP gene are associated with scrapie susceptibility.

Nine amino acid polymorphisms of the sheep PrP gene have been described, at codons 112, 136, 137, 138, 141, 151, 154, 171 and 211 [1–6, 10–11, 17, 20–22, 28–29]. Polymorphisms at codons 112, 137, 138, 141, 151 and 211 are rare, and have not been found to be associated with disease phenotype in natural or experimental scrapie [3, 21, 28–29]. A polymorphism at codon 136 has been found to be associated with scrapie susceptibility in both experimental [11–12] and natural scrapie [15, 21]. Studies have shown that a polymorphism at codon 171 is associated with susceptibility to experimental scrapie in Cheviot sheep [12] and natural scrapie in Suffolk sheep [30]. The association between scrapie susceptibility and polymorphism at codon 154 is currently unclear, but evidence suggests that histidine at codon 154 is associated with low susceptibility to scrapie in some breeds of sheep [9, 28]. Researchers have found that the PrP allelic variant alanine/arginine/arginine (ARR) at codons 136, 154 and 171 is associated with resistance to scrapie in several breeds [1, 3, 6, 12, 15, 17, 21]. In Suffolk sheep, in which the PrP allele valine/arginine/glutamine (VRQ) at codons 136, 154 and 171 is rare or absent, the wild-type PrP allele alanine/arginine/glutamine (ARQ) is associated with susceptibility to scrapie [7, 8, 10, 16, 18, 30].

The current sheep population in Mongolia is estimated to be over 13.8 million. The native breed, Khalkh, comprises about 90% of Mongolian sheep. This breed possesses desirable features such as has hardiness and prolificacy, with good meat, fat and wool characteristics. Crossbreeding between Khalkh and imported sheep started in the 1930s, in an effort to develop tastier meat and higher quality wool [13, 14]. The PrP genotypes of native sheep in Central Asia have not previously been studied. Therefore, we examined the PrP genotypes of 271 sheep raised in Mongolia, including Khalkh (the native breed) and 3 recently developed crossbreeds (Yeroo, Orkhon and Khangai). We examined the sheep for polymorphisms of the PrP gene associated with scrapie susceptibility.

MATERIALS AND METHODS

Sheep: A total of 271 sheep from 4 breeds (Khalkh, Yeroo, Orkhon and Khangai) raised in central Mongolia were used in this study. These included 172 Khalkh sheep (native breed) raised in Tuv and Uvurkhangai districts, 35 Yeroo sheep raised in Selenge prefecture, 35 Orkhon sheep raised in Selenge prefecture, and 29 Khangai sheep raised in Selenge prefecture. The Yeroo, Orkhon and Khangai breeds are crossbreeds of Khalkh sheep and non-native breeds.

DNA extraction and amplification: Blood from 271 sheep was collected using heparin as an anticoagulant. High-molecular-mass DNA was isolated from blood using QIAGEN kits (Hilden, Germany). The PrP gene, including the entire 794-bp open reading frame (ORF), was amplified in 50-μl reaction volumes by polymerase chain reaction (PCR), using 0.5 to 1 μg genomic DNA in standard PCR buffer (Perkin Elmer, Norwalk, CT) and 25 to 50 pmol each of 2 primers (SPrP-1, 5'-CATCATGGTGAAAAGCCA-CATAGGC-3'; SPrP-2, 5'-GAAAACAGGAAGGT-TGCCC CTATCC-3'), as described by Ikeda *et al.* [19]. PCR conditions were as follows: initial step, 95°C for 9 min;

50 cycles, consisting of denaturation at 94°C for 0.5 min, annealing at 55°C for 0.5 min, and extension at 72°C for 1 min; final step, 72°C for 7 min. After PCR amplification, the products were electrophoresed in 0.7% agarose gels containing ethidium bromide (0.5 μg/m*l*), and visualized under ultraviolet radiation. Then, the primers were removed using a Centricon 100 micro-concentrator (Amicon, Bedford, MA), and 1 to 5 μ*l* of the concentrated PCR product was used for direct sequencing.

Cloning and DNA Sequencing: For cloning and DNA sequencing, 794-bp fragments of the PrP allelic variants were amplified by PCR. Amplified DNA fragments were phosphorylated with T4 Kinase (Takara, Kyoto, Japan) and inserted into the *Eco*RI site of the Bluecript SK$^+$ plasmid vector (Stratagene, La Jolla, CA) according to standard protocols [23]. The purified PCR products and the cloned DNA fragments in pBluescript SK$^+$ were directly sequenced using an ABI PRISM Dye Terminator Cycle Sequencing Ready FS Kit with a 373S autosequencer (Perkin-Elmer, Norwalk, CT). The DNA sequence data were analyzed using GENETYX-MAC software (Software Development Co., Ltd., Tokyo, Japan).

Restriction fragment length polymorphism (RFLP) analysis: To examine polymorphism at codon 127, DNA was amplified using the following primers: SPrP1, 5'-CATCATGGTGAAAAAGCCACATAGGC-3'; SP2, 5'-CACTTGGTTGGGGTAACGGTAC-3'. Using 10 U of the restriction enzymes *Ava*II and *Hae* III (Pharmacia Biotech), 20 μ*l* of the PCR product was digested. The primers SP1 (5'-TTGTGGCTACATGCG GGAAG-3') and SPrP5 (5'-ATAAGCCTGGGATTCTCTCT-3') and the restriction enzyme *Sau*3AI were used to examine polymorphism at codon 171. The primers SP1 (5'-TTGGTGGCTACATGCTGGGAAG-3') and SPrP5 (5'-ATAAGCCTGGGATTCTCTCT-3') and the restriction enzyme *Alu*I were used for codon 189. The samples were incubated for 3 to 5 hr at 37°C, and approximately 5-μ*l* aliquots of both digested and undigested PCR products were electrophoresed on 2.5% agarose gels. The fractionation patterns in the gels were visualized under UV light and photographed.

RESULTS

PrP genotypes and allelic variants: We observed well-known dimorphisms at codons 112, 136, 154 and trimorphism at codon 171. Eight different allelic variants were found. Using these 8 allelic variants, we found a total of 16 different PrP genotypes. Table 1 shows the genotype and allelic variant frequencies of the 271 sheep examined.

Khalkh: The 172 Khalkh sheep were found to have the

Table 1. Frequency of PrP genotypes and allelic variants of 4 sheep breeds from Central Mongolia

PrP genotype	Khalkh		Yeroo		Orkhon		Khangai	
	No	%	No	%	No	%	No	%
MARQ/MARQ	86	50.0	17	48.5	13	37.0	15	51.7
MARQ/TARQ	31	18.0	4	11.4	7	20.0	2	6.9
MARQ/MARR	20	11.6	8	22.8	8	22.8	9	31.0
MARQ/MARH	16	9.3			1	2.9		
TARQ/MARR	5	2.9			1	2.9		
TARQ/MARH	4	2.3			1	2.9		
TARQ/TARQ	4	2.3	1	2.9				
MARH/MARH	2	1.2			1	2.9		
MARH/TARH	2	1.2						
MARR/MARR	1	0.6	2	5.7			2	6.9
MARK/MARK	1	0.6						
MARQ/MVRQ			1	2.9	2	5.7		
MARR/MVRQ			1	2.9				
MARH/MAHQ			1	2.9				
MARR/MAHQ					1	2.9		
TARQ/MAHQ							1	3.5
Total	172	100	35	100	35	100	29	100
PrP allelic variant								
MARQ	239	69.5	47	67.1	44	62.9	41	70.7
TARQ	48	14.0	6	8.6	9	12.8	3	5.2
MARR	27	7.8	13	18.6	10	14.3	13	22.4
MARH	26	7.5	1	1.4	4	5.7		
TARH	2	0.6						
MARK	2	0.6						
MVRQ			2	2.9	2	2.9		
MAHQ			1	1.4	1	1.4	1	1.7
Total	344	100	70	100	70	100	58	100

greatest variation, with 11 PrP genotypes and 6 PrP allelic variants. These animals were polymorphic at codons 112 and 171. Variation was not detected at codons 136 and 154. The most frequent PrP genotype was MARQ/MARQ (50.0%), followed by MARQ/TARQ (18.0%) and MARQ/MARR (11.6%). The PrP allelic variant with the highest frequency was MARQ (69.5%), followed by TARQ (14.0%) and MARR (7.8%). Only one animal (0.6%) had the genotype MARR/MARR.

Yeroo: Eight PrP genotypes and 6 PrP allelic variants were found in the 35 Yeroo sheep. The most frequent genotype was MARQ/MARQ (48.5%), followed by MARQ/MARR (22.8%) and MARQ/TARQ (11.4%). The PrP allelic variant with the highest frequency was MARQ (67.1%), followed by MARR (18.6%) and TARQ (8.6%).

Orkhon: Nine PrP genotypes and 6 PrP allelic variants were found in the 35 Orkhon sheep. The most frequent PrP genotype was MARQ/MARQ (37.0%), followed by MARQ/MARR (22.8%) and MARQ/TARQ (20.0 %). The PrP allelic variant with the highest frequency was MARQ (62.9%), followed by MARR (14.3%) and TARQ (12.8%).

Khangai: Five PrP genotypes and 4 PrP allelic variants were found in the 29 Khangai sheep, but the 136V and 171H alleles were not found. The most frequent PrP genotype was MARQ/MARQ (51.7%), followed by MARQ/MARR (31.0%) and MARQ/TARQ (6.9%). The PrP allelic variant with the highest frequency was MARQ (70.7%), followed by MARR (22.4%) and TARQ (5.2%).

Distribution of PrP codon 136 and 171 genotypes associated with scrapie susceptibility among the Mongolian sheep breeds: Because scrapie in sheep is most strongly associated with polymorphisms at codons 136 and 171 of the PrP gene, these codons were examined in great detail in the present study. Table 2 shows the distribution of genotypes of PrP codons 136 and 171 among the Mongolian sheep breeds used in this study. The genotypes VQ/VQ, AQ/AQ and AR/AR correlate with high susceptibility, moderate susceptibility, and low susceptibility to scrapie, respectively. The genotype AQ/AQ was found in 70.3% of Khalkh sheep, 62.8% of Yeroo sheep, 57.1% of Orkhon sheep, and 62.1% of Khangai sheep. The genotype AR/AR was found in 0.6% of Khalkh sheep, 5.7% of Yeroo sheep, and 6.9% of Khangai sheep. The genotype AR/AR was not found in Orkhon sheep. The genotype AQ/VQ was found in 2.9% of Yeroo sheep and 5.7% of Orkhon sheep. The genotype AR/VQ was found in 2.9% of Yeroo sheep. The 136V allele, which correlates with high susceptibility to scrapie, was found in the crossbreeds Yeroo and Orkhon, but not in Khalkh or Khangai sheep. The 171H allele was found in 14.0% of Khalkh sheep, 8.6% of Orkhon sheep and 2.9% of Yeroo sheep, but not in Khangai sheep. At codons 136 and 171, 1.8% of the sheep had the genotype AR/AR (associated with low susceptibility to scrapie) and 66.8% had the AQ/AQ genotype (associated with moderate susceptibility to scrapie).

Novel amino acid polymorphisms detected in this study: In Khalkh, Yeroo and Orkhon sheep, we found the following novel polymorphisms: codon 127, valine (V; nucleotides GTC) and serine (S; AGC); codon 171, lysine (K; AAG); codon 189, leucine (L; CTA) and arginine (R; CGA) (Fig. 1 and Fig. 2).

In 27 Khalkh sheep, we detected a G→A nucleotide substitution at the first position of codon 127 (changed the amino acid from glycine [G] to serine) and a G→T nucleotide substitution at the second position of codon 127 (changed the amino acid from glycine to valine). In 6 Yeroo sheep and one Orkhon sheep, we detected a G→A nucleotide substitution at the first position of codon 127 (changed the amino acid from glycine to serine).

Figure 1 shows RFLP analysis results that demonstrate novel polymorphisms at codon 127. Digestion of wild-type (127G/G) PCR products (496 bp) with *Ava*II produced 451-bp and 45-bp fragments. Digestion of 127G/V PCR products with *Ava*II produced 4 fragments: 451, 382, 69 and 45 bp. Digestion of wild-type (127G/G) PCR products with *Hae*III produced 5 fragments: 69, 141, 174, 37 and 75 bp. Digestion of 127S/S PCR products with *Hae*III produced 4 fragments: 69, 141, 211 and 75 bp. Digestion of 127G/S PCR products with *Hae*III produced 6 fragments: 69, 141, 174, 211, 37 and 75 bp.

Table 2. Distribution of genotypes of PrP codons 136 and 171 associated with scrapie susceptibility among Mongolian sheep breeds

PrP genotype	Khalkh		Yeroo		Orkhon		Khangai	
136 / 171	No	%	No	%	No	%	No	%
AQ/AQ**	121	70.3	22	62.8	20	57.1	18	62.1
AQ/AR	25	14.5	8	22.8	10	28.6	9	31.0
AR/AR***	1	0.6	2	5.7			2	6.9
AQ/VQ*			1	2.9	2	5.7		
AR/VQ*			1	2.9				
AQ/AH	20	11.6	1	2.9	2	5.7		
AH/AH	4	2.4			1	2.9		
AK/AK	1	0.6						
Total	172	100	35	100	35	100	29	100

* High susceptibility to scrapie.
** Moderate susceptibility to scrapie.
*** Low susceptibility to scrapie.

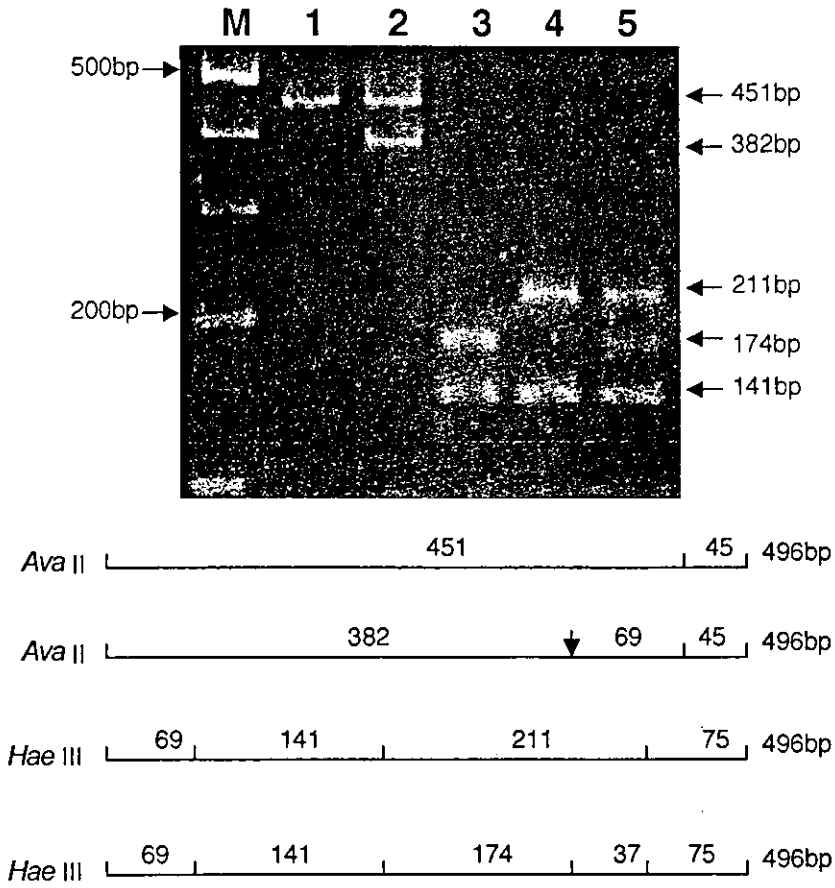

Fig. 1. Novel polymorphisms at codon 127, as indicated by RFLP analysis. Lane M: 100-bp DNA ladder marker. Lane 1: 127G/G PCR product was digested with *Ava*II (451- and 45-bp fragments). Lane 2: 127G/V PCR product was digested with *Ava*II (451-, 382-, 69- and 45-bp fragments). Lane 3: 127G/G PCR product was digested with *Hae*III (69-, 141-, 174-, 37- and 75-bp fragments). Lane 4: 127S/S PCR products were digested with *Hae*III (69-, 141-, 211- and 75-bp fragments). Lane 5: 127G/S PCR products were digested with *Hae*III (69-, 141-, 174-, 211-, 37- and 75-bp fragments). In 2.5% agarose gel, 69-, 45-, 37- and 75-bp fragments were not clearly detectable. The vertical arrow indicates newly generated restriction sites at codon 127.

In one Khalkh sheep, we detected a C→A nucleotide substitution at the first position of codon 171 (changed the amino acid from glutamine [Q] to lysine). In 15 Khalkh sheep, we detected an A→T nucleotide substitution at the second position of codon 189 (changed the amino acid from glutamine to leucine) and an A→G nucleotide substitution at the second position of codon 189 (changed the amino acid from glutamine to arginine). In 2 Orkhon and one Yeroo sheep, we detected an A→T nucleotide substitution at the second position of codon 189 (changed the amino acid from glutamine to leucine). None of the above novel polymorphisms were not found in Khangai sheep.

Figure 2 shows RFLP analysis results that demonstrate novel polymorphisms at codons 171 and 189. Digestion of 171Q/Q (wild type) PCR product (302 bp) with *Sau*3AI produced 2 fragments: 125 and 177 bp. The enzyme *Sau*3AI failed to digest 171K/K PCR product (302-bp product remained intact). The enzyme *Alu*I failed to digest 189Q/Q (wild-type) PCR product (302-bp product remained intact). Digestion of 189L/L with *Alu*I produced 2 fragments: 182 and 120 bp.Digestion of 189Q/L and 189Q/R PCR product with *Alu*I produced 3 fragments: 302, 182 and 120 bp.

Two silent substitutions, A→C at the first position of codon 231 (arginine) and C→G at the third position of codon 237 (leucine), were found in all breeds. Polymorphisms previously detected in sheep at codons 137, 138, 141, 151 and 211 [3–5, 22, 28, 29] were not found in the present study.

DISCUSSION

The results of this study show the relative genotype fre-

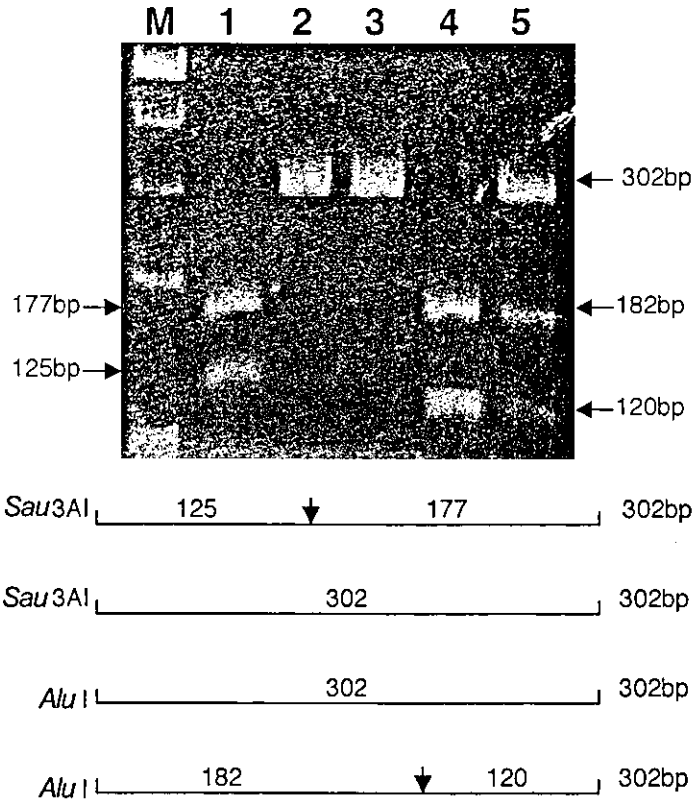

Fig. 2. Novel polymorphisms at codons 171 and 189, as indicated by RFLP analysis. Lane M: 100-bp DNA ladder marker. Lane 1: 171Q/Q PCR product was digested with *Sau*3AI (125- and 177-bp fragments). Lane 2: *Sau*3AI failed to digest 171K/K PCR product (intact 302-bp product). Lane 3: *Alu*I failed to digest 189Q/Q PCR product (intact 302-bp product). Lane 4: 189L/L PCR product was digested with *Alu*I (182- and 120-bp fragments). Lane 5: 189Q/L PCR products were digested with *Alu*I (302-, 182- and 120-bp fragments). The vertical arrows indicate newly generated restriction sites at codons 171 and 189.

quencies of 4 codons (112, 136, 154 and 171) of the PrP gene in 4 sheep breeds (Khalkh, Yeroo, Orkhon and Khangai) found in central Mongolia. This is the first report of PrP genotype frequencies for these breeds of Mongolian sheep. In this study, 16 different PrP genotypes and 8 different PrP allelic variants of the PrP gene were found. Three PrP genotypes (MARQ/MARQ, MARQ/TARQ and MARQ/MARR) and 3 PrP allelic variants (MARQ, TARQ and MARR) were found in all 4 breeds. These results are comparable to those obtained in studies of sheep in Japan and France [19–21]. PrP dimorphisms at codons 112, 136 and 154 and a trimorphism at codon 171 resulted in 6 variant alleles (MARQ, TARQ, MVRQ, MAHQ, MARR and MARH) that have previously been found in Suffolk and Corriedale sheep. The genotype TARQ has previously been found in Suffolk sheep but not in Corriedale sheep [19]. In another study, 3 allellic variants of the PrP gene (MARQ, TARQ and MARR) were found in Suffolk sheep [20]. Five polymorphic variants (MARQ, TARQ, MVRQ, MAHQ and MARR) have been found at codons 112, 136, 154 and 171 of the PrP gene in Ile-de-France and Romanov sheep in France [21].

In the present study, the 154H allele was found in the 3 crossbreeds but not in the Khalkh breed. In one study, this allele was found in 9 scrapie-free Romanov sheep in France [21]. In another study, only a few healthy Suffolk sheep were found to carry the PrP allele MAHQ, and no scrapie-affected Suffolk sheep were found to carry this allele; association of this allele with scrapie is unclear [19]. We found the 136V allele, which correlates with high scrapie susceptibility, in Yeroo and Orkhon sheep, but we did not find this allele in Khalkh or Khangai sheep. In a related study in Ireland, only one of the 188 pedigree Suffolk rams examined had variation at codon 136 [24]. In 3 flocks in the USA (159 healthy purebred Suffolk sheep), the alleles 136A and 136V were found in 97% and 3% of the sheep, respectively [31]. The fact that we did not find the alleles 136A and 136V in Khalkh sheep, which are native to Mongolia, suggests that

they were inherited from foreign breeds during the development of the 3 new breeds.

We found the novel polymorphisms 127V, 127S, 171K, 189L and 189R in the native Mongolian breed Khalkh. The only novel polymorphisms found in Yeroo and Orkhon sheep were 127S and 189L, which were not found in Khangai sheep. It appears that the novel polymorpisms found only in Khalkh sheep are unique to this breed. However, it is not known whether these polymorphisms are associated with scrapie susceptibility.

The allele consisting of VRQ at codons 136, 154 and 171, respectively, is rare or absent in Suffolk sheep [7, 8, 10, 16, 30] and the Mongolian sheep we examined. The allele consisting of ARQ at these 3 codons is associated with scrapie susceptibility [7, 10, 16, 18, 31]. The proportion of Mongolian sheep carrying the171Q/Q genotype is comparable to those of Suffolk sheep from the USA and Japan [24]. However, the Khalkh and Orkhon breeds had much lower frequencies (0.6% and 0%, respectively) of the 171R/R genotype (which is associated with low scrapie susceptibility) than all Suffolk sheep that have previously been studied (ranged from 4.2% to 48%) [24]. Thus, Khalkh and Orkhon sheep may be more genetically susceptible to scrapie than Suffolk sheep.

There have been no reports of cases of scrapie in Mongolia, but the present results suggest that the majority of Mongolian sheep are potentially genetically susceptible to scrapie. Therefore, we examined brain tissues from 10 sheep with neurological symptoms (4 Khalkh sheep from Tuv prefecture, 3 Khangai from Selenge prefecture, and 3 Orkhon sheep from Selenge prefecture). However, results of Western blot analysis of these tissues were negative for the scrapie form of the prion protein (PrP^{Sc}) (data not shown). Conclusive determination as to whether scrapie exists in Mongolia will require the examination of many sheep with neurological symptoms.

This study was limited to sheep from central Mongolia, but studies of sheep from other regions of Mongolia are currently being conducted. The findings of these studies may provide information that can be used to select scrapie-resistant sheep for breeding.

ACKNOWLEDGEMENTS. This work was partly supported by a grant from the Ministry of Health and Welfare of Japan, from Ministry of Agriculture, Forestry and Fisheries of Japan and Grant-in-Aid for Science Research from the Ministry of Education, Science and Culture of Japan (12460130, 12575030, 10556069).

REFERENCES

1. Belt, P.B.G.M., Muileman, I.H., Schreuder, B.E.C., Bos-de Ruijter, J., Gielkens, A.L.J. and Smits, M.A. 1995. Identification of five allelic variants of the sheep PrP gene and their association with natural scrapie. *J. Gen. Virol.* **76**: 509–517.
2. Belt, P.B.G.M., Bossers, A., Schreuder, B.E.C. and Smits, M.A. 1996. PrP allelic variants associated with natural scrapie, pp. 294–305. *In*: Bovine Spongiform Encephalopathy; the BSE Dilemma Gibbs, C.J. Jr. ed., Springer, New York, N.Y.
3. Bossers, A., Screuder, B.E.C., Muileman, I.H., Belt, P.B.G.M. and Smits, M.A. 1996. PrP genotype contributes to determining survival times of sheep with natural scrapie. *J. Gen. Virol.* **77**: 2669–2673.
4. Bossers, A., Harders, F.L. and Smits, M.A. 1999. PrP genotype frequencies of the most dominant sheep breed in a country free from scrapie. *Arch. Virol.* **144**: 829–834.
5. Bossers, A., de Vries, R. and Smits, M.A. 2000. Susceptibility of sheep for scrapie as assessed by *in vitro* conversion of nine naturally occurring variants of PrP. *J. Virol.* **74**: 1407–1414.
6. Clouscard, C., Beaudry, P., Elsen, J.M., Milan, D., Dussaucy, M., Bounneau, C., Schelcher, Chatelain, J., Launay, J.M. and Laplanche, J.L. 1995. Different allelic effects of the codons 136 and 171 of the prion protein gene in sheep with natural scrapie. *J. Gen. Virol.* **76**: 2097–2101.
7. Dawson, M. 1997. PrP genotyping (scrapie gene testing) as an aid to the control of scrapie. *State Vet. J.* **7**: 16–17.
8. Dawson, M., Hoinville, L., Hosie, B.D. and Hunter, N. 1998. Guidance on the use of PrP genotyping as an aid to the control of clinical scrapie. *Vet. Rec.* **142**: 623–625.
9. Elsen, J.M., Amigues, Y., Schelcher, F., Ducrocq, V., Andreoletti, O., Eychenne, F.,Vu Tien Khang, J., Poivey, J..P., Lantier, F. and Laplanche, J.L. 1999. Genetic susceptibility and transmission factors in scrapie: detailed analysis of an epidemic in a closed flock of Romanov. *Arch. Virol.* **144**: 431–445.
10. Goldmann, W., Hunter, N., Foster, J.D., Salbaum, J.M., Beyreuther, K. and Hope, J. 1990. Two alleles of a neural protein gene linked to scrapie in sheep. *Proc. Natl. Acad. Sci. U.S.A.* **87**: 2476–2480.
11. Goldmann, W., Hunter, N., Benson, G., Foster, J.D. and Hope, J. 1991. Different scrapie-associated fibril proteins (PrP) are encoded by lines of sheep selected for different alleles of the Sip gene. *J. Gen. Virol.* **72**: 2411–2417.
12. Goldmann, W., Hunter, N., Smith, G., Foster, J.D. and Hope, J. 1994. PrP genotype and agent effects in scrapie: change in allelic interaction with different isolates of agent in sheep, a natural host of scrapie. *J. Gen. Virol.* **75**: 989–995.
13. Gombojav, A. 1997. pp. 1–10. Health Programs for Raising Khalkh lambs in Central Mongolia. Mongolian Agricultural University, Ulaanbaatar, Mongolia.
14. Gonchigjav, Z. 2000. pp. 46–49, 143–177. Mongolian sheep. Mongolian Agricultural University, Ulaanbaatar, Mongolia.
15. Hunter, N., Goldmann, W., Benson, G., Foster, J.D. and Hope, J. 1993. Swaledale sheep affected by natural scrapie differ significantly in PrP genotype frequencies from healthy sheep and those selected for reduced incidence of scrapie. *J. Gen. Virol.* **74**: 1025–1031.
16. Hunter, N., Goldmann, W., Smith, G. and Hope, J. 1994. The association of a codon 136 PrP gene variant with the occurrence of natural scrapie. *Arch. Virol.* **137**: 171–177.
17. Hunter, N., Foster, J.D., Goldmann, W., Stear, M.J., Hope, J. and Bostock, C. 1996. Natural scrapie in a closed flock of Cheviot sheep occurs only in specific PrP genotypes. *Arch. Virol.* **141**: 809–824.
18. Hunter, N., Moore, L., Hosie, B.D., Dingswall, W.S. and Greig, A. 1997. Association between natural scrapie and PrP genotype in a flock of Suffolk sheep in Scotland. *Vet. Rec.* **140**: 59–63.
19. Ikeda, T., Horiuchi, M., Ishiguro, N., Muramatsu, Y., Kai-Uwe, G.D. and Shinagawa, M. 1995. Amino acid polymorphisms of PrP with reference to onset of scrapie in Suffolk and

Corriedale sheep in Japan. *J. Gen. Virol.* **76**: 2577–2581.
20. Ishiguro, N., Shinagawa, M., Onoe, S., Yamanouchi, K. and Saito, T. 1998. Rapid analysis of allelic variants of the sheep PrP gene by oligonucleotide probes. *Microbiol. Immunol.* **42**: 579–582.
21. Laplanche, J.L., Chatelain, J., Westaway, D., Thomas, S., Dussaucy, M., Brugere-Picoux, J. and Launay, J.M. 1993. PrP polymorphisms associated with natural scrapie discovered by denaturing gradient gel electrophoresis. *Genomics* **15**: 30–37.
22. Loftus, B., Monks, E., Hanlon, J., Weavers, E. and Rogers, M. 1999. Prion protein genotypes of Suffolk-type sheep representative of natural scrapie in Ireland. *Ir. Vet. J.* **52**: 81–85.
23. Maniatis, T., Fritsh, E.F. and Sambrook, J. 1982. Molecular Cloning: a Laboratory Manual. Cold Spring Harbor Laboratories, Cold Spring Harbor, New York.
24. O'Doherty ,E., Aherne, M., Ennis, S., Weavers, E., Hunter, N., Roche, J.F. and Sweeney, T. 2000. Detection of polymorphisms in the prion protein gene in a population of Irish Suffolk sheep. *Vet. Rec.* **146**: 335–338.
25. Prusiner, S.B. 1982. Novel proteinaceous infectious particles cause scrapie. *Science* **216**: 136–144.
26. Prusiner, S.B. 1991. Molecular biology of prion diseases. *Science* **252**: 1515–1522.
27. Prusiner, S.B. 1997. Prion diseases and the BSE crisis. *Science* **278**: 245–251.
28. Thorgeirsdotteir, S., Sigurdarson, S., Thorisson, H.M., Georgsson, G. and Palsdottir, A. 1999. PrP gene polymorphism and natural scrapie in Icelandic sheep. *J. Gen. Virol.* **80**: 2527–2534.
29. Tranulis, M.A., Osland, A., Bratberg, B. and Ulvund, M.J. 1999. Prion protein gene polymorphism in sheep with natural scrapie and healthy controls in Norway. *J. Gen. Virol.* **80**: 1073–1077.
30. Westaway, D., Zuliani, V., Mirenda Cooper, C., Da Costa, M., Neuman, S., Jenny, A.L., Detwiler, L. and Prusiner, S.B. 1994. Homozygosity for prion protein alleles encoding glutamine-171 renders sheep susceptible to natural scrapie. *Genes. Dev.* **8**: 959–969.
31. Yuzbasiyan-Gurkan, V., Krehbiel, J.D., Cao, Y. and Venta, P.J. 1999. Development and usefulness of new polymerase chain reaction-based tests for detection of different alleles at codons 136 and 171 of the ovine prion protein gene. *Am. J. Vet. Res.* **7**: 884–887.

Cellular Prion Protein Promotes *Brucella* Infection into Macrophages

Masahisa Watarai,[1] Suk Kim,[1] Janchivdorj Erdenebaatar,[1] Sou-ichi Makino,[1] Motohiro Horiuchi,[2] Toshikazu Shirahata,[1] Suehiro Sakaguchi,[3] and Shigeru Katamine[3]

[1]*Department of Applied Veterinary Science and* [2]*Research Center for Protozoan Diseases, Obihiro University of Agriculture and Veterinary Medicine, Hokkaido 080-8555, Japan*

[3]*Department of Molecular Microbiology and Immunology, Nagasaki University Graduate School of Biomedical Sciences, Nagasaki 852-8523, Japan*

Abstract

The products of the *Brucella abortus virB* gene locus, which are highly similar to conjugative DNA transfer system, enable the bacterium to replicate within macrophage vacuoles. The replicative phagosome is thought to be established by the interaction of a substrate of the VirB complex with macrophages, although the substrate and its host cellular target have not yet been identified. We report here that Hsp60, a member of the GroEL family of chaperonins, of *B. abortus* is capable of interacting directly or indirectly with cellular prion protein (PrP^C) on host cells. Aggregation of PrP^C tail-like formation was observed during bacterial swimming internalization into macrophages and PrP^C was selectively incorporated into macropinosomes containing *B. abortus*. Hsp60 reacted strongly with serum from human brucellosis patients and was exposed on the bacterial surface via a VirB complex–associated process. Under in vitro and in vivo conditions, Hsp60 of *B. abortus* bound to PrP^C. Hsp60 of *B. abortus*, expressed on the surface of *Lactococcus lactis*, promoted the aggregation of PrP^C but not PrP^C tail formation on macrophages. The PrP^C deficiency prevented swimming internalization and intracellular replication of *B. abortus*, with the result that phagosomes bearing the bacteria were targeted into the endocytic network. These results indicate that signal transduction induced by the interaction between bacterial Hsp60 and PrP^C on macrophages contributes to the establishment of *B. abortus* infection.

Key words: Hsp60 • type IV secretion • macropinocytosis • intracellular replication • brucellosis

Introduction

Brucella species are Gram-negative bacteria that cause brucellosis with pathological manifestations of arthritis, endocarditis, and meningitis as well as undulant fever in humans and abortion and infertility in numerous domestic and wild mammals (1). The bacterium is endemic in many developing countries and is responsible for large economic losses and chronic infections in humans (2). *Brucella* species are facultative intracellular pathogens that survive within a variety of cells, including macrophages. The virulence of these species and the establishment of chronic infection are thought to be due essentially to their ability to avoid the killing mechanisms within macrophages (3). However, the molecular mechanisms accounting for these properties are not understood completely.

Recent studies with nonprofessional phagocyte HeLa cells have confirmed these observations, showing that *Brucella* inhibits phagosome–lysosome fusion and transits through an intracellular compartment that resembles autophagosomes. Bacteria replicate in a different compartment, containing protein markers normally associated with the endoplasmic reticulum, as shown by confocal microscopy and immunogold electron microscopy (4, 5).

Brucella internalizes into macrophages by swimming on the cell surface with generalized membrane ruffling for several minutes, a process termed "swimming internalization," after which the bacteria are enclosed by macropinosomes (6). In this period, the phagosomal membrane continues to

Address correspondence to Masahisa Watarai, Department of Applied Veterinary Science, Obihiro University of Agriculture and Veterinary Medicine, Inada-cho, Obihiro-shi, Hokkaido 080-8555, Japan. Phone: 81-155-49-5387; Fax: 81-155-49-5386; E-mail: watarai@obihiro.ac.jp

J. Exp. Med. © The Rockefeller University Press • 0022-1007/2003/07/5/13 $8.00
Volume 198, Number 1, July 7, 2003 5–17
http://www.jem.org/cgi/doi/10.1084/jem.20021980

maintain a dynamic state. Lipid raft–associated molecules, such as glycosylphosphatidylinositol (GPI)*-anchored proteins, GM1 gangliosides, and cholesterol, have been shown to be selectively incorporated into macropinosomes containing *Brucella abortus*. In contrast, late endosomal marker lysomal-associated membrane protein (LAMP)-1 and host cell transmembrane proteins are excluded from the macropinosomes. The disruption of lipid rafts on macrophages markedly inhibits the VirB-dependent macropinocytosis and intracellular replication (6). These results indicated that the entry route of *B. abortus* into the macrophages determined the intracellular fate of the bacteria that was modulated by lipid rafts (6, 7).

The operon coding for export mechanisms specializing in transferring a variety of multimolecular complexes across the bacterial membrane to the extracellular space or into other cells has been described (8). These complexes, named type IV secretion systems, are also found in *B. abortus* (*virB* genes; 9–11). This operon comprises 13 open reading frames that share homology with other bacterial type IV secretion systems involved in the intracellular trafficking of pathogens. Type IV secretion systems export three types of substrates: (a) DNA conjugation intermediates, (b) the multisubunit pertussis toxin, and (c) monomeric proteins including primase, RecA, the *Agrobacterium tumefaciens* VirE2 and VirF proteins, and the *Helicobacter pylori* CagA protein (8). However, the substrates of the VirB secretion system of *B. abortus* and the target of the effector in host cells remain undefined.

In this study, we investigated the effector protein secreted by the type IV secretion systems and its receptor on the host plasma membrane. Our results implied that heat shock protein Hsp60 of *B. abortus* had an effector-like function, which was expressed on the bacterial surface by the type IV secretion–associated manner. The cellular prion protein (PrP^C) was identified as a receptor for the Hsp60. This receptor–ligand interaction regulates the establishment of *B. abortus* infection.

Materials and Methods

Reagents. Gentamicin, protein A–Sepharose 4B beads, and 4′,6-diamidino-2-phenylindole (DAPI) were obtained from Sigma-Aldrich. Ni-NTA agarose beads were obtained from QIAGEN. Alexa Fluor 594-streptavidin, Cascade blue goat anti–rabbit IgG, and Texas Red goat anti–rat IgG were obtained from Molecular Probes, Inc. Rhodamine goat anti–rabbit or mouse IgG was obtained from ICN Pharmaceuticals. Anti–*B. abortus* polyclonal rabbit serum, aerolysin, and anti- PrP^C biotin-labeled mouse monoclonal antibody have been described (6, 12). Anti–mouse CD48 rat monoclonal antibody MRC OX-78 was obtained from Serotech. Anti–*Escherichia coli* GroEL mouse monoclonal antibody 9A1/2 was obtained from Calbiochem. Anti-Hsp60 rabbit polyclonal antibody was obtained from MBL International Corporation. Anti–glucose-6-phosphate dehydrogenase (G6PDH) goat polyclonal antibody was obtained from Cortex Biochem. *Brucella*-infected human, cattle, and sheep sera have been described (13). Anti–LAMP-1 rat monoclonal antibody 1D4B was obtained from the Developmental Studies Hybridoma Bank of the Department of Pharmacology and Molecular Sciences, Johns Hopkins University School of Medicine and the Department of Biology, University of Iowa.

Bacterial Strains and Media. All *B. abortus* derivatives were from 544 (ATCC23448), smooth virulent *B. abortus* biovar 1 strains. Ba598 (544 Δ*virB4*), Ba600 (544 GFP$^+$), and Ba604 (Δ*virB4* GFP$^+$) have been described (6, 14). *B. abortus* strains were maintained as frozen glycerol stocks and cultured on Brucella broth (Becton Dickinson) or Brucella broth containing 1.5% agar. Kanamycin was used at 40 μg/ml.

Construction of An In-Frame Deletion Mutant of virB2. pMAW24 (Δ*virB2*) was constructed by cloning two PCR fragments into SalI/SacI-cleaved pSR47s (14). Fragment 1 was a 1,609-bp SalI-BglII fragment spanning a site located 1,609 nucleotides upstream of the 5′ end of *virB2* to 6 nucleotides downstream from the 5′ end and was amplified by PCR using primers 5′-GTCGACATGACAGGCATATTTCAACGC-3′ (SalI site underlined) and 5′-AGATCTTTTCATGATCTTTATTCCTAA-3′ (BglII site underlined; nucleotide positions 1 and 1,614 are available from GenBank/EMBL/DDBJ under accession no. AF226278, respectively; reference 10). Fragment 2 was a 1,600-bp BamHI-SacI fragment spanning the region starting 6 nucleotides upstream of the 3′ end of *virB2* to a position 1,594 nucleotides downstream from the 3′ end and was amplified using primers 5′-GGATCCAGGTAAAGGGACACAGATCAT-3′ (BamHI site underlined) and 5′-GAGCTCCATCCCGCTTGCCTGCGC-GGA-3′ (SacI site underlined; nucleotide positions 1,921 and 3,526 are available from GenBank/EMBL/DDBJ under accession no. AF226278, respectively; reference 10). pMAW24 (Δ*virB2*) was introduced into *E. coli* DH5α (λ*pir*) and then the plasmid was transferred into *B. abortus* 544 by electroporation (Gene Pulser; Bio-Rad Laboratories). Isolation of in-frame deletion mutant by the positive selection for sucrose resistance has been described (14).

pMAW25 (*virB2*$^-$) was constructed by cloning a PCR fragment into SalI/BamHI-cleaved pBBR1MCS-2 (15). The 707-bp EcoRI-BamHI PCR fragment spanned a site located 369 nucleotides upstream of the 5′ end of *virB2* to a position 21 nucleotides downstream from the 3′ end (10) and was amplified using the primers 5′-GTCGACGTTATAGCGGCGGGCGGCGAC-3′ (SalI site underlined) and 5′-GGATCCGTTGTCATGATCT-GTGTCCCT-3′ (BamHI site underlined).

Cell Culture. Bone marrow–derived macrophages from female BALB/c, C57BL/6, Ngsk, or Zrch PrP^C-deficient mice (16, 17), and PrP^C transgenic Ngsk PrP^C-deficient mice (18) were prepared as previously described (6, 14). After culturing in L cell–conditioned medium, the macrophages were replated for use by lifting cells in PBS on ice for 5 to 10 min, harvesting cells by centrifugation, and resuspending cells in RPMI 1640 containing 10% fetal bovine serum. The macrophages were seeded ($2–3 \times 10^5$ per well) in 24-well tissue culture plates for all assays.

Immunofluorescence Microscopy. Detection of intracellular bacteria, macropinosome formation, and fluorescence-labeled molecules by fluorescence microscopy have been described (6). In brief, *B. abortus* strains were grown to A600 = 3.2 in Brucella broth and used to infect mouse bone marrow–derived macrophages for various lengths of time at a multiplicity of infection of

*Abbreviations used in this paper: DAPI, 4′,6-diamidino-2-phenylindole; G6PDH, glucose-6-phosphate dehydrogenase; GPI, glycosylphosphatidylinositol; LAMP, lysomal-associated membrane protein; NPC1, Niemann-Pick type C1 gene; PrP, prion protein; PrP^C, cellular PrP; WASP, Wiskott-Aldrich syndrome protein.

20. Infected cells were fixed in periodate-lysine-paraformaldehyde containing 5% sucrose for 1 h at 37°C. Samples were washed three times in PBS and wells were successively incubated three times for 5 min in blocking buffer (2% goat serum in PBS) at room temperature.

All antibody-probing steps were for 1 h at 37°C. Samples were washed three times in PBS for 5 min and then permeabilized in −20°C methanol for 10 s. After incubating three times for 5 min with blocking buffer, samples were stained with each primary antibody. After washing three times for 5 min in blocking buffer, samples were stained simultaneously with each secondary antibody. Samples were placed in mounting medium and visualized by fluorescence microscopy.

100 macrophages were examined per coverslip to determine the total number of intracellular bacteria, macropinosome formation, and total number of bacteria within macropinosomes (6).

Determination of Efficiency of Bacterial Uptake and Intracellular Growth by Cultured Macrophages. To determine uptake of bacteria, mouse bone marrow–derived macrophages were infected with *B. abortus*. After 0, 5, 15, 25, and 35 min incubation at 37°C, macrophages were washed once with medium and incubated with 30 μg/ml gentamicin for 30 min. Macrophages were then washed three times with fresh medium and lysed with distilled water. CFUs were determined by serial dilutions on Brucella plates. Percentage protection was determined by dividing the number of bacteria surviving the assay by the number of bacteria in the infectious inoculum, as determined by viable counts.

To determine intracellular growth of bacteria, the infected macrophages were then washed once with medium and incubated with 30 μg/ml gentamicin. At different time points, cells were washed and lysed with distilled water and the number of bacteria was counted on plates of a suitable dilution (6).

Ni-NTA Agarose Pull-Down and Immunoprecipitation Assay. A fusion protein of Hsp60 tagged with six histidine residues at the NH_2 terminus was constructed using the QIAexpress system with pQE30 plasmid (QIAGEN). The fusion Hsp60 protein was purified by Ni-NTA chromatography.

For the pull-down assay, Ni-NTA agarose beads–bound Hsp60 (20 μg/ml) were added to 1 ml macrophage lysate (~10^6 cells) prepared with lysis buffer (10 mM Tris-HCl, pH 7.6, 5 mM EDTA, 50 mM NaCl, 30 mM sodium pyrophosphate, 50 mM NaF, 1% Triton X-100, 0.1% SDS, 4 μg/ml leupeptin, 1 mM PMSF; reference 19), and the mixture was incubated at 37°C for 20 min. Ni-NTA agarose beads–bound PrP^C (20 μg/ml; reference 20) were added to 1 ml purified Hsp60 solution (20 μg/ml), and the mixture was incubated at 37°C for 20 min.

For immunoprecipitation assay, 20 μg/ml Hsp60 added to 1 ml macrophage lysate was incubated at 37°C for 20 min. The sample was then immunoprecipitated with the anti-PrP^C antibody and incubated at 4°C overnight. Protein A–Sepharose beads were added to the sample and incubated at room temperature for 1 h. Each protein or antibody (20 μg/ml) was added in reaction solution and incubated for 20 min before pull-down or immunoprecipitation for binding inhibition.

The precipitates were washed with PBS and analyzed by immunoblotting with either anti-Hsp60 or anti-PrP^C, and silver staining was performed using 2D-Silver Stain II (Daiichi Pure Chemicals).

Expression of Hsp60 on Lactococcus Lactis. pMAW30 (*B. abortus* $Hsp60^+$) or pMAW31 (*E. coli* $Hsp60^+$) was constructed by cloning a PCR fragment into KpnI/SacI- or SacI-cleaved pSECE1, which is a vector for the secretion of foreign protein to the cell surface of *L. lactis* (21). The 1,640-bp KpnI-SacI or 1,647-bp SacI PCR fragment spanned the *hsp60* gene of *B. abortus* (22) or *E. coli* (23) and was amplified using the primers 5′-GGTACCATGGCTGCAAAAGACGTAAAA-3′ (KpnI site underlined) and 5′-GAGCTCTTAGAAGTCCATGCCGCCCAT-3′ (SacI site underlined), or 5′-GAGCTCATGGCAGCTAAAGACGTAAAA-3′ (SacI site underlined) and 5′-GAGCTCTTACATCATGCCGCCCATGCC-3′ (SacI site underlined). Transformation of *L. lactis* IL1403 was performed according to the method of Holo and Nes (24).

Hsp60 Localization on Bacteria. Bacteria were grown to A600 = 3.2 in broth, collected by centrifugation, and fixed in 4% paraformaldehyde. Expression of Hsp60 on the *B. abortus* or *L. lactis* surface was confirmed by immunofluorescence microscopy with anti-Hsp60 monoclonal antibody (25). Immunofluorescence staining of permeabilized bacteria was performed as previously described (25).

ELISA. The ability of PrP^C to bind to Hsp60 on *L. lactis* was measured as follows. A 50-μl aliquot of ~10^8 *L. lactis* was placed into 96-well immuno plates (Nunc) and incubated at room temperature for 2 h. The sample was then removed and the wells were washed twice with PBS-0.05% Tween 20. 50 μl macrophage lysate (200 μg/ml) were added and the plate was incubated at 37°C for 1 h. The amount of bound PrP^C was determined by ELISA with anti-PrP^C antibody.

Time Lapse Video Microscopy. Bone marrow–derived macrophages were plated in Lab-Tek Chambered coverglass (Nunc) and incubated overnight in RPMI 1640 containing 10% FBS at 37°C in 5% CO_2. 2×10^6/ml bacteria were added to the chamber and then the chamber was placed on a heated microscope stage set to 37°C for observation using an Olympus IX70 inverted phase microscope with 100× UPlanApo lens fitted with phase contrast optics. The bacteria were allowed to settle passively onto the macrophages and images were captured over a 30-min period. The images were captured every 15 s using a cooled CCD camera (CoolSNAP; Roper Scientific) and processed using Openlab software (Improvision) on a Power Macintosh G4 computer.

Virulence In Mice. Virulence was determined by quantitating the survival of the strains in the spleen after 10 d. Groups of five mice were injected intraperitoneally with ~10^4 CFUs of brucellae in 0.1 ml saline. At 10 d after infection, their spleens were removed and homogenized in saline. Tissue homogenates were serially diluted with PBS and plated on Brucella agar to count the number of CFUs in each spleen.

Results

Tail Formation of PrP^C with Swimming Internalization of B. abortus. Our previous results showed that GPI-anchored proteins were selectively incorporated into macropinosomes containing *B. abortus* (Fig. 1; reference 6). To investigate further the membrane sorting process, the distribution of GPI-anchored proteins during swimming internalization of *B. abortus* was analyzed. Aerolysin from *Aeromonas hydrophila*, which binds to the GPI moiety of GPI-anchored proteins on the cell surface (26), was used as probe for the detection of GPI-anchored proteins. At 5 min after infection, aggregation of aerolysin-labeled GPI-anchored proteins showing tail-like formation was colocalized with swimming bacteria on the macrophage surface (Fig. 1). In contrast, no aggregation of CD48, which is a GPI-anchored protein, was observed at the same time

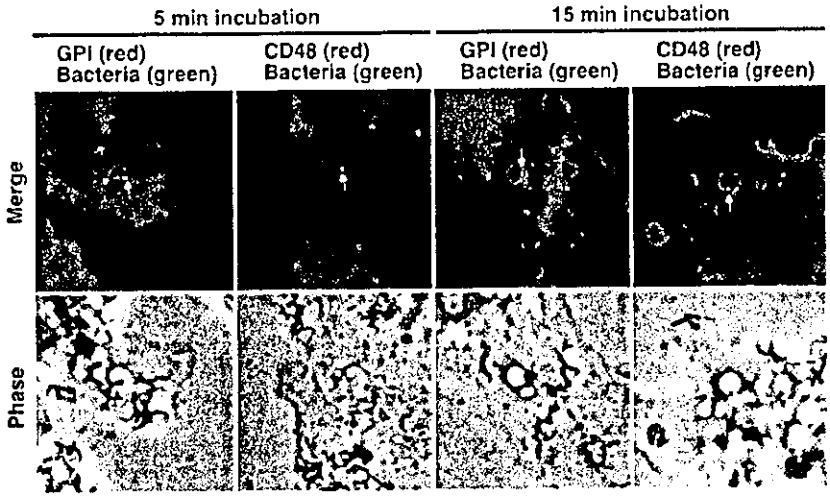

Figure 1. Tail formation of GPI-anchored proteins on the site of swimming internalization. Bone marrow–derived macrophages were incubated with *B. abortus* for 5 or 15 min, and GPI-anchored proteins were localized by immunofluorescence as described in Materials and Methods. Merged images of the GFP (green) and TRITC (red) channels up and down with phase contrast images of the same field are shown. Cells were probed with aerolysin for GPI-anchored proteins and with anti-CD48. White arrows point to bacteria and blue arrow points to tail-like aggregation of GPI-anchored proteins.

point (Fig. 1). Similar results were obtained for other GPI-anchored proteins, such as CD55 (unpublished data). However, when one GPI-anchored protein, PrP^C, was tested, colocalization of aggregated PrP^C tail and swimming bacteria was observed (Fig. 2 A). Sometimes, several PrP^C tails were observed from a single bacterium (Fig. 2 A). PrP^C was also incorporated into macropinosomes containing wild-type strain, but not *virB4* mutant, after 15 min incubation (Fig. 2 A).

To obtain the ratio of PrP^C tail formation, colocalization of PrP^C tail and internalized bacteria was quantitated microscopically at various times of incubation. *virB4* mutant was rapidly internalized, with most bacteria internalized before further incubation, but the internalization of wild-type strain was delayed (Fig. 2 B). Wild-type strain, but not *virB4* mutant, was present in macropinosomes transiently (Fig. 2 C). The kinetics and degree of association of the PrP^C tail with internalized wild-type strain showed maximal association after 5 min incubation (Fig. 2 D). The maximal association of PrP^C with phagosomes containing wild-type strain was observed after 15 min incubation (Fig. 2 E). In contrast, colocalization of PrP^C with *virB4* mutant was much less pronounced (Fig. 2, D and E). These results suggested that bacterial products secreted by the type IV system might aggregate PrP^C specifically and form tail structures during swimming internalization of *B. abortus*.

Surface Exposure of Hsp60 on B. abortus. To investigate bacterial factors associated with PrP^C tail formation, immunodominant proteins were examined by immunoblotting with human brucellosis sera, which recognized a major protein (60 kD) and two minor proteins (30~25 kD; Fig. 3 A). In a previous report (22), immunodominant Hsp60 reacted with sera from mice experimentally infected with *B. abortus*. Therefore, the 60-kD protein was expected to be Hsp60. To confirm this, purified Hsp60 of *B. abortus* was analyzed by immunoblotting with sera from human and animal brucellosis. As expected, Hsp60 reacted with serum from human, cattle, and sheep with naturally acquired brucellosis (Fig. 3 B). Mutant strains (Δ*virB2* and Δ*virB4*) also had immunoreactive Hsp60 (Fig. 3 A). To examine if Hsp60 was secreted into the external medium, culture supernatant of *B. abortus* was analyzed by immunoblotting. Immunoreactive proteins were not detected in culture supernatant (unpublished data). However, surface-exposed Hsp60 on wild-type strain, but not *virB2* and *virB4* mutants, was detected by immunofluorescence staining with anti-Hsp60 antibody (Fig. 3 C). Because introduction of complementing plasmid into each mutant restored surface expression of Hsp60, the expression of Hsp60 on the bacterial surface associates with the type IV secretion system (Fig. 3 C).

To demonstrate that, as above, the presence of Hsp60 on the bacterial surface did not result from wholesale relocalization of cytoplasmic leakage, a control experiment was performed. Surface exposure of G6PDH was determined by immunofluorescence microscopy. Antibody against G6PDH failed to react with bacterial cell surfaces. As it was not certain that the control antibody was able to react with bacterial cells in the immunofluorescence experiment, the antibody was used to probe bacteria in the presence or absence of permeabilization by hypotonic lysozyme treatment (25). Antibody against G6PDH reacted with permeabilized bacteria, but failed to react with bacterial cell surface (Fig. 3 D). Therefore, the surface exposure of Hsp60 is not caused by cytoplasmic leakage.

Interaction of PrP^C with Hsp60 of B. abortus. Because Hsp60 expressed on the bacterial surface by the type IV secretion system was most likely interacting with the target cell, we tested Hsp60 for its ability to bind to PrP^C on macrophages by pull-down assay with Hsp60 or PrP^C beads. Analysis of the precipitated proteins by immunoblotting with anti-PrP^C or Hsp60 antibody showed that a 29-kD PrP^C was associated with Hsp60, but not beads alone (Fig. 4, A and B). To confirm this association, Hsp60 was added to macrophage lysate and the proteins in the mixture were then immunoprecipitated with anti-PrP^C antibody. The

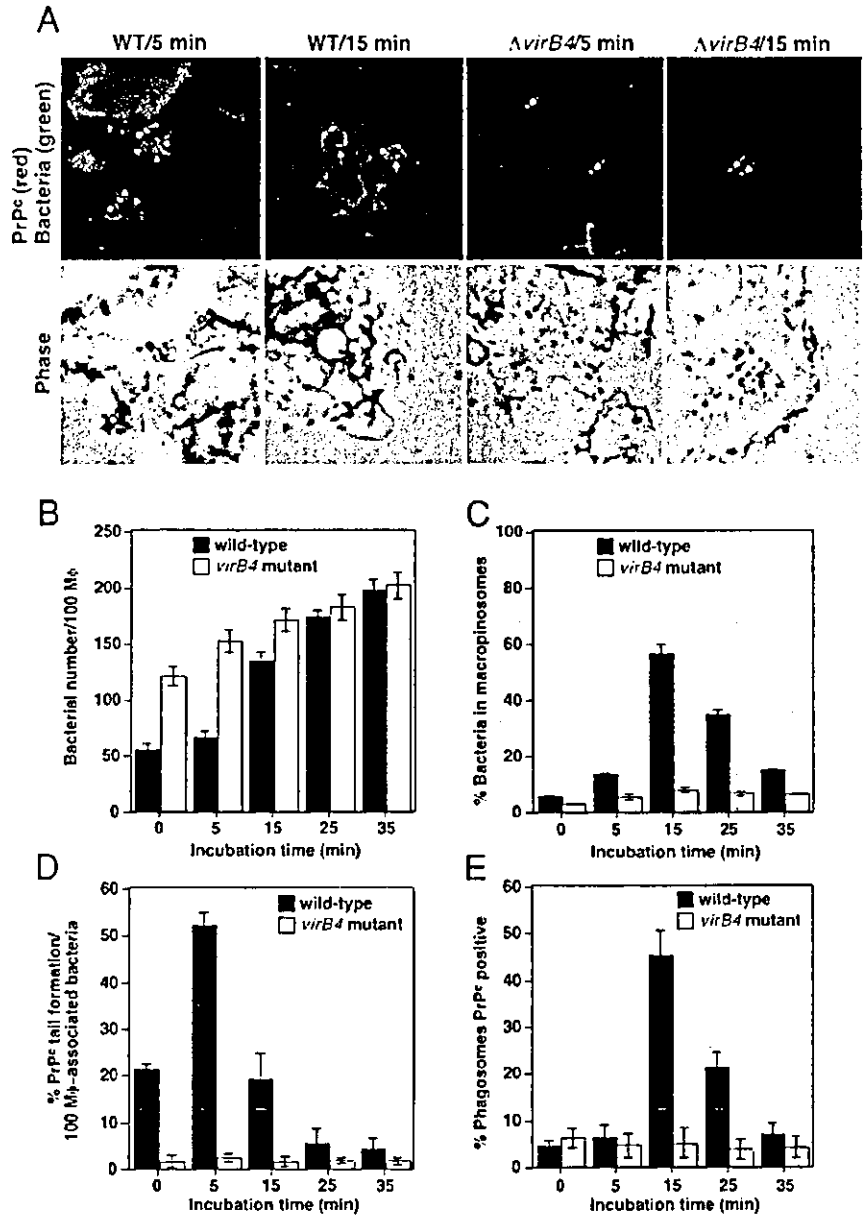

Figure 2. PrI^{R} tail formation at the site of swimming internalization. (A) Macrophages were incubated with *B. abortus* for 5 or 15 min, and PrI^{C} were localized by immunofluorescence as described in Materials and Methods. Merged images of the GFP (green) and TRITC (red) channels up and down with phase contrast images of the same field are shown. White arrows point to bacteria and blue arrows point to tail-like aggregation of PrI^{C}. (B–E) Wild-type (solid bars) or *virB4* mutant (open bars) were deposited onto macrophages and then incubated for the periods of time indicated. Uptake (B), macropinosome formation (C), PrI^{C} tail formation (D), or PrI^{R} positive phagosomes (E) was quantified as described in Materials and Methods. % PrI^{R} tail formation or % phagosomes PrI^{R} positive refers to the percentage of bacteria that showed costaining with the PrI^{C} tail or PrI^{R}-included phagosomes. 100 macrophages (B and C) or 100 bacteria (D and E) were examined per coverslip. Data are the average of triplicate samples from three identical experiments, and the error bars represent the standard deviation.

precipitated proteins were analyzed by immunoblotting with anti-Hsp60 antibody. The precipitates contained Hsp60 (Fig. 4 B). Because the anti-Hsp60 antibody did not recognize macrophages Hsp60, the antibody showed specific for bacterial Hsp60 (Fig. 4 B). This Hsp60 and PrP^{C} association was inhibited by the addition of anti-Hsp60 polyclonal antibody, purified Hsp60, or PrP^{C} (Fig. 4, A and B). These results indicated that the interaction between Hsp60 and PrP^{C} would be specific. The precipitated proteins were also analyzed by silver staining. The precipitates contained two major bands (60 and 29 kD) and two weak minor bands (74 and 27 kD; Fig. 4 C). These results suggested that Hsp60 bound to PrP^{C} mostly, but there is possibility that Hsp60 might interact indirectly with PrP^{C} mediated by other cellular components.

To further characterize Hsp60, distribution of Hsp60 in *B. abortus*–infected macrophages was analyzed by immunofluorescence microscopy. At 5 or 15 min after infection, Hsp60 colocalized with only the bacterial surface and was not detected in macrophage membrane or cytoplasm (Fig. 4 D).

To investigate if Hsp60 exposed on bacterial surface could aggregate PrP^{C} on macrophages, macrophages were infected with *L. lactis* expressing Hsp60 of *B. abortus* on its surface (Fig. 5 B), and then PrI^{C} was detected by immunofluorescence microscopy. After 5 min incubation, PrP^{C}

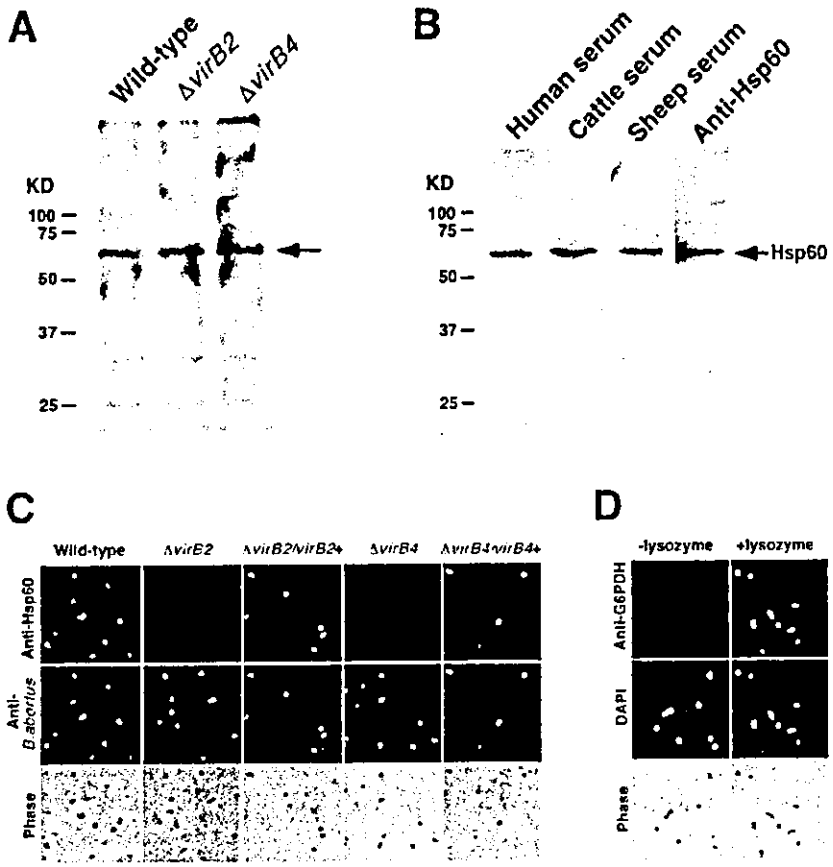

Figure 3. VirB complex–dependent surface expression of immunodominant Hsp60. Immunoblot analysis of whole cell lysates with serum from human brucellosis (A) and of purified Hsp60 with indicated serum (B). (C) Labeling of bacteria grown in vitro with antibody specific for Hsp60. Fluorescence microscopy of stained wild-type, *virB2*, or *virB4* mutant, and complemented strain for each mutant, with anti-Hsp60 (top) or anti-*B. abortus* (middle) and phase contrast microscopy of the corresponding microscopic fields (bottom) are shown. (D) Localization of G6PDH on permeabilized *B. abortus* by immunofluorescence microscopy. Bacteria were probed with anti-G6PDH (top) and stained for DNA with DAPI (middle) in either the absence (−lysozyme) or the presence (+lysozyme) of lysozyme, and phase contrast microscopy of the corresponding microscopic fields (bottom) are shown.

accumulated around internalized Hsp60$^+$ *L. lactis* but not Hsp60$^-$ *L. lactis* (Fig. 5 A). Quantitative data showed that >70% of *L. lactis* expressing Hsp60 colocalized with PrP^C at all time points (Fig. 5 D). PrP^C tail formation was not observed with either Hsp60$^+$ or Hsp60$^-$ *L. lactis*. *L. lactis* was seeded on the wells of a microtiter plate, macrophage lysate was added, and then binding activity was measured by ELISA with anti-PrP^C antibody. The binding of PrP^C to Hsp60 on the *L. lactis* surface was detected but not with Hsp60$^-$ *L. lactis* (Fig. 5 C). *L. lactis* expressing Hsp60 of *E. coli* also colocalized with PrP^C at all time points, but the percentage of colocalization was lower than Hsp60 of *B. abortus* (Fig. 5, C–E). These results suggested that Hsp60 expressed on the bacterial surface promoted accumulation of PrP^C, but is not sufficient for PrP^C tail formation.

Effect of PrP^C Deficiency on B. abortus Infection. To investigate the role of PrP^C on *B. abortus* infection, several phenotypes of *B. abortus* virulence were tested by using macrophages from Ngsk PrP^C-deficient mice (16). Time lapse videomicroscopy was used to follow the internalization of *B. abortus* by macrophages from parent or Ngsk PrP^C-deficient C57BL/6 mice. After contact of macrophages with *B. abortus*, bacteria showed swimming internalization in macrophages from parent mice (Fig. 6 A). The swimming of the bacteria on the macrophage surface lasted for several minutes with generalized plasma membrane ruffling before eventual enclosure in macropinosomes (Fig. 6 A). Contact of *B. abortus* with macrophages from Ngsk PrP^C-deficient mice, in contrast, resulted in much smaller ruffling that was restricted to the area near the bacteria. The ruffles associated with internalization of bacteria resulted in a more rapid uptake than observed for macrophages from parent mice (Fig. 6 B). 5 min after deposition on the macrophages from parent mice, *B. abortus* showed generalized actin polymerization around the site of bacterial binding, which could be observed by either phalloidin staining or phase contrast microscopy (Fig. 6 C). Macrophages from Ngsk PrP^C-deficient mice showed primarily small regions of phalloidin staining at sites of bacterial binding (Fig. 6 C).

The differences in rate of phagocytosis and macropinosome formation for parent or Ngsk PrP^C-deficient mice were quantitated microscopically at various times of incubation. The kinetics of bacterial internalization and macropinosome formation in macrophages from parent C57BL/6 mice were almost identical to those observed for macrophages from BALB/c mice (Figs. 2, B and C, and 7, A–C). Internalization of wild-type *B. abortus* into macrophages from Ngsk PrP^C-deficient mice, in contrast, was much quicker and macropinosome formation was hardly detectable (Fig. 7, D–F). The internalized wild-type strain did

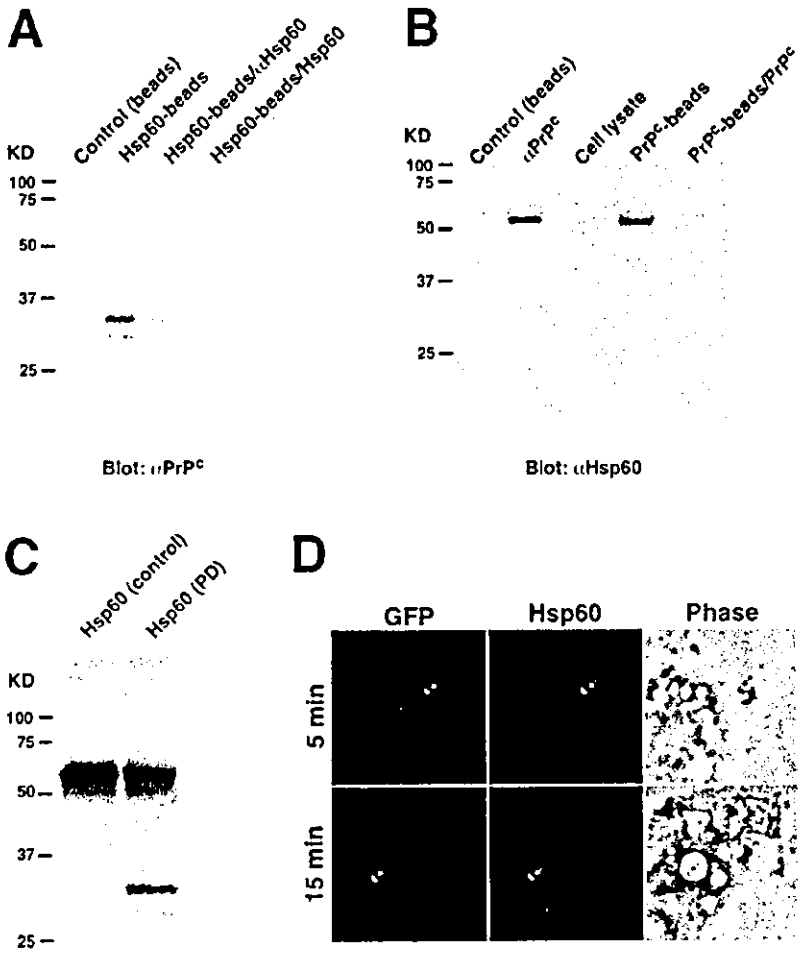

Figure 4. Binding of Hsp60 to PrP^C. (A) Demonstration of affinity of Hsp60 for PrP^C by pull-down assay with Hsp60-coated beads. Control was assessed with beads only, the addition of anti-Hsp60 antibody, or purified Hsp60. Precipitates were analyzed by immunoblotting with anti-PrP^C antibody. (B) Cell lysate or immunoprecipitates with anti-PrP^C antibody and affinity of PrP^C for Hsp60 by pull-down assay with PrP^C-coated beads was analyzed by immunoblotting with anti-Hsp60 antibody. Control was assessed with beads only, or the addition of purified PrP^C. (C) Silver staining of precipitates by pull-down assay. Samples were purified with Hsp60 (control) and precipitates of pull-down with Hsp60-coated beads (PD). (D) Labeling of internalized bacteria in macrophages with antibody specific for Hsp60. Macrophages were incubated with *B. abortus* for 5 or 15 min, and Hsp60 were localized by immunofluorescence as described in Materials and Methods. Fluorescence microscopy of stained GFP-expressed wild-type strain with anti-Hsp60 and phase contrast microscopy of the corresponding microscopic fields are shown. Arrows point to bacteria.

not replicate in the macrophages from Ngsk PrP^C-deficient mice (Fig. 7 G). Macrophages from parent and Ngsk PrP^C-deficient mice showed no significant difference in the internalization, macropinosome formation, and intracellular replication of *virB4* mutant (Fig. 7, A–F and H). In macrophages from Ngsk PrP^C-deficient mice, wild-type strain failed to block phagosome maturation as shown by colocalization of phagosomes containing the bacteria and the late endocytic marker, LAMP-1, at 35 min after infection (Fig. 8, A and C). In contrast, wild-type strain prevented phagosome-lysosome fusion, and therefore phagosomes containing wild-type strain do not have LAMP-1 in macrophages from parent mice (Fig. 8, A and B).

To determine if this defect in intracellular replication of *B. abortus* correlates with an inability to establish infection in the host, we experimentally infected parent or PrP^C-deficient mice with *B abortus*. Many bacteria were recovered from the spleen of BALB/c and C57BL/6 mice infected with wild-type strain at 10 d after infection, but few bacteria were recovered from PrP^C-deficient mice, based on the number of CFUs in each spleen (Fig. 7 I). As previously reported (14), fewer bacteria were recovered from the spleen of three mice strains infected with *virB4* mutant (Fig. 7 I). These results suggested that replicative phagosome formation and proliferation in mice of *B. abortus* required the uptake pathway associated with PrP^C.

Several of the phenotypes ascribed to Ngsk PrP^C-deficient mice are most likely caused by up-regulation of prion protein (PrP)-like protein doppel rather than by ablation of PrP^C (27). To investigate the involvement of doppel expression on *B. abortus* infection, Zrch PrP^C-deficient mice (17), with no up-regulation of doppel, were used for infection assay. The results showed that phenotypes of Zrch PrP^C-deficient mice were almost the same as Ngsk PrP^C-deficient mice on *B. abortus* infection (Fig. 7 G). In addition, PrP^C transgenic Ngsk PrP^C-deficient mice were successfully rescued from the inhibition of bacterial intracellular growth (Fig. 7 G). Therefore, doppel expression was not involved in *B. abortus* infection.

Discussion

In this study, we have shown that Hsp60 of *B. abortus*, secreted on the bacterial surface by the type IV secretion

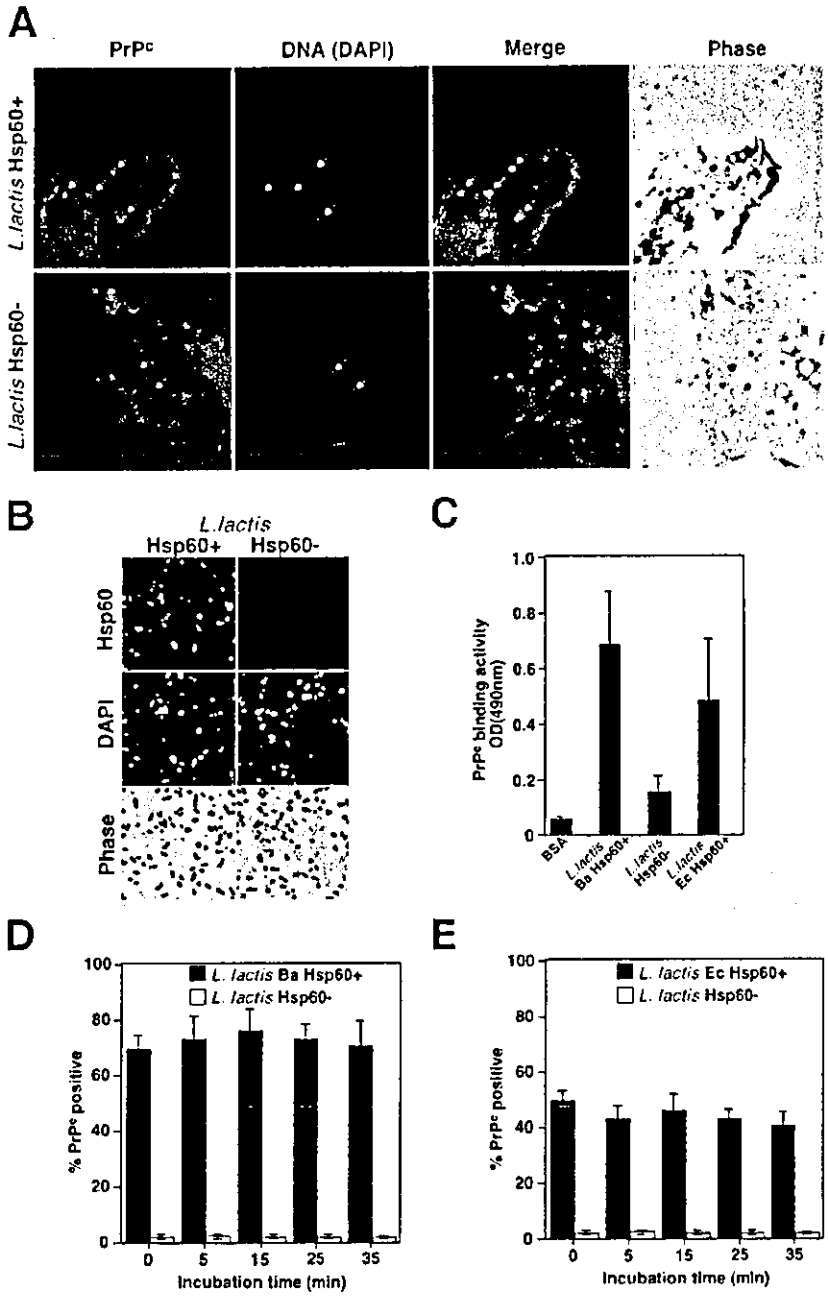

Figure 5. Aggregation of PrP^{c} by Hsp60 expressed on the surface of *L. lactis*. Macrophages were incubated with surface $Hsp60^{+}$ (top) or $Hsp60^{-}$ (bottom) *L. lactis* for 5 min, and PrP^{c} was localized by immunofluorescence as described in Materials and Methods. Phase contrast microscopy of the corresponding microscopic fields are shown. Bacteria (shown by arrows) were stained with DAPI. (B) Labeling of *L. lactis* grown in vitro, with antibody specific for Hsp60. Fluorescence microscopy of stained surface $Hsp60^{+}$ or $Hsp60^{-}$ *L. lactis* with anti-Hsp60 (top) or DAPI (middle) and phase contrast microscopy of the corresponding microscopic fields (bottom) are shown. (C) PrP^{c}-binding activity. Measurement of PrP^{c}-binding activity was performed by ELISA (refer to Materials and Methods). (D and E) Macrophages were incubated with surface $Hsp60^{+}$ (solid bars) or $Hsp60^{-}$ (open bars) *L. lactis* for the indicated time, and association of PrP^{c} was determined by immunofluorescence microscopy. Hsp60 of *B. abortus* (D) or *E. coli* (E) is expressing on *L. lactis* surface. % PrP^{c} positive refers to percentage of bacteria that showed costaining with PrP^{c}. 100 bacteria were examined per coverslip. Data are the average of triplicate samples from three identical experiments, and the error bars represent the standard deviation.

system–associated manner, interacted directly or indirectly with PrP^{c}, and that the interaction contributed to establish *B. abortus* infection. The cellular function of PrP^{c} is unclear. Our results in this study provide a novel aspect of PrP^{c} function as a receptor for an intracellular pathogen. Hsp60s, a member of the GroEL family of chaperonins in *E. coli*, is widely distributed and conserved between prokaryotes and mammals (28). Hsp60 proteins have been recognized as immunodominant antigens of many microbial pathogens, including *B. abortus* (22, 29). Hsp60s are believed to reside in the cytoplasm (30). However, surface-exposed Hsp60 has been reported in *Legionella pneumophila* and shown to be involved in pathogenicity (31). Presumably, Hsp60 of *L. pneumophila* binds to unknown receptors on nonprofessional phagocyte HeLa cells, initiating actin polymerization and endocytosis of the bacterium into an early endosome (32). But the role of surface-exposed Hsp60 in professional phagocytes, such as macrophages, is still unclear. As *L. pneumophila* has a type IV secretion system, surface expression of Hsp60 of *L. pneumophila* might